



Copyright © Aalborg University 2025



AAU Energy Aalborg University

Aalborg University http://www.aau.dk

AALBORG UNIVERSITY

STUDENT REPORT

Title:

Performance of an Electrified Hot Potassium Carbon Capture System under Varying Operating Conditions

Theme:

Modeling and analysis of a point source carbon capture system

Project Period:

Autumn Semester 2025

Project Group:

TEPE4

Participant(s):

Mads Bluhme Jeppesen

Supervisor(s):

Xiaoti Cui

Page Numbers: 48

Date of Completion:

September 21, 2025

Mads Bluhme Jeppesen Aalborg University

Abstract:

In this project, a point-source hot potassium carbonate (HPC) carbon capture system, based on CapSol's End-of-Pipe system was modelled in Aspen Plus V12.1. The aim of the project was to find the operating conditions in which the HPC system performs the best, as well as publicise information that enables easier comparison of this system to similar carbon capture systems.

The model was a rate-based, steady state model and was validated by comparing the reaction equilibrium to experimental data. The model diverged by 14% to 17% from the data and had a maximum temperature of 120 °C at places reactions are simulated.

It was concluded that the HPC system can function on electric power and cold utility, along with some makeup water and absorbent, with an efficiency at 24 wt.% CO₂ (approx 16 mol%) flue gas of 915 kJ/kg CO₂ power and 993 kJ/kg CO₂ cold utility, with significant efficiency drops at low CO₂ concentrations.

Other investigations include how the regenerator, absorber and lean flash box pressure affect the system, as well as the sensitivity of the flash box pressures with regards to the system capture rate.

The content of this report is freely available, but publication (with reference) may only be pursued due to agreement with the author.

By accepting the request from the fellow student who uploads the study group's project report in Digital Exam System, you confirm that all group members have participated in the project work, and thereby all members are collectively liable for the contents of the report. Furthermore, all group members confirm that the report does not include plagiarism.

Preface

To preface this project, I would like to thank my supervisor Xiaoti Cui for his continued guidance throughout this project.

Readers guide

Literature references are made using the Harvard numeric method. Tools used for this project are as following:

- Aspentech, Aspen Plus V12.1 Simulation tool
- Microsoft 365, Excel Data processing
- JGraph Ltd, Diagrams.net Flowchart maker
- The Matplotlib Development Team, Matplotlib Graph maker
- Overleaf LaTeX editor

Contents

1	Intr	oduction	3	
2	Stat	e of the Art	4	
	2.1	Liquid Chemical Absorption Technologies	4	
		2.1.1 Liquid Amine Technologies	4	
		2.1.2 Potassium Carbonate Technologies	5	
		2.1.3 Chilled Ammonia Technologies	6	
	2.2	Solid Adsorption Technologies	6	
	2.3	Cryogenic Technologies	7	
	2.4	Membrane Technologies	8	
	2.5	Pre-Combustion Technologies	8	
	2.6	Conclusion to State of the Art	9	
3	Prol	olem Statement	10	
4 Model Setup				
	4.1	System Overview	11	
		4.1.1 Flash Boxes	13	
		4.1.2 Absorber	14	
		4.1.3 Regenerator	14	
		4.1.4 Recuperation Cooler	15	
		4.1.5 CO2 Cooler	15	
	4.2	Chemistry	16	
	4.3	Model setup in Aspen Plus	17	
		4.3.1 Basis of the Model	17	
		4.3.2 Model Chemistry	18	
		4.3.3 Aspen model	20	
	4.4	Validation of Model	21	
5	Resi	ults and discussion	25	
-	5.1	Utility Requirements	25	
	5.2	Sensitivity Analysis	28	

Contents		vi

Re	ferer	ices		44
6	Con	clusion	l	42
	5.3	Table (of Recommended Settings	41
			ture Rate and System Efficiency	
		5.2.4	Effects of Flash Box Pressure and Steam Temperature on Cap-	
		5.2.3	Effect of Flue Gas Mass Flow on System Efficiency	35
			ciency	32
		5.2.2	Effect of Absorber and Regenerator pressure on System Effi-	
		5.2.1	Effects of Various Flue Gas Compositions on System Efficiency	28

Contents 1

Nomenclature

Abbreviation	Description
aq	Aqueous solution
CC	Carbon Capture
CCC	Cryogenic Carbon Capture
CAPEX	Capital Expenditure
COP	Coefficient of Performance
DAC	Direct Air Capture
EoP	End-of-Pipe
EU	European Union
HPC	Hot Potassium Carbonate
1	Liquid
ln	Natural Logarithm
MVR	Mechanical Vapor Recompression
pН	potential of hydrogen
PSC	Point Source Capture
wt.%	Weight Percentage
MEA	Monoethanolamine
MOF	Metal-Organic Framework
TRL	Technology Readiness Level

Sub- and superscripts	Description
a,b,c	order of reaction
cooling	Cooling stream
cold	Low temperature input
combined	Temperature of both inputs once combined
cond	Condensate
hot	High temperature input
n	fit constant
pre	pre-exponential factor
vap@T	Vapor at T temperature
CO_2	CO ₂

Contents 2

Symbol	Description	Unit
ΔΗ	Change in Enthalpy	kJ
A,B,C,D	Reaction specific constants (equilibrium equation)	-
A_{pre}	Pre-exponential Factor	-
c_p	Specific Heat Capacity at Constant Pressure	<u>kJ</u> K∙kg
E	Activation energy	kJ/kmol
k	Rate Coefficient	$\frac{1}{\sec'}$, $\frac{1}{secmol'}$, $\frac{1}{secmol^2}$
K_eq	Equilibrium Constant	-
m	Mass Flow	kg/s
r	Reaction rate	<u>kmol</u> m³:sec k1
R	Ideal Gas Constant	[™] kJ K·kmol
T	Temperature	°C
P	Pressure	kPa
Q	Thermal Energy	kJ

Chapter 1

Introduction

Since the first Industrial Revolution, the global output of greenhouse gases, especially carbon dioxide, has been increasing each decade [1]. This almost continuous increase has resulted in the current output of carbon dioxide (CO₂), currently being estimated to be over 700 times higher than it was just 200 years ago [2]. This is a troubling trend, as it is well documented that CO₂, along with other greenhouse gases, are responsible for climate change [3][4][5]. Curbing this increase in emissions is, therefore, necessary if the effects of climate change are to be limited. This is further outlined by the international treaty on climate change named The Paris Agreement [6], which is currently signed by 196 parties, that concludes that the global temperature increase, compared to before the first Industrial Revolution, shall be "well below 2 °C" and preferably below 1.5 °C [7].

One method of reducing emissions is point source carbon capture (PSC), which captures CO₂ before it leaves the chimney of the factories and power plants that produce it. This is particularly important in industries, that cannot remove CO₂ emissions by electrifying the process or where electrification is impossible, such as cement plants, chemical plants and power plants. Once captured, the CO₂ can either be stored to directly prevent it from entering the atmosphere or utilized for green fuels or in chemical plants, as a replacement for fossil fuels, to indirectly prevent further emissions.

However, carbon capture (CC) is currently a highly energy consuming process, making it both expensive and less climate friendly. New CC technologies that have higher efficiencies are, therefore, desirable, to reduce the carbon footprints of the systems and to incentivize companies to invest in carbon capture technologies. The aim of this report will be to investigate one such upcoming technology and provide insight into its workings, energy and capture efficiency, and discern in what use cases this system might outperform comparable state of the art CC technologies.

Chapter 2

State of the Art

As there are large differences in how different carbon capture technologies function, a single technology will be chosen for analysis in this report. To select a technology a state of the art analysis is made to ascertain what technology would be most relevant.

2.1 Liquid Chemical Absorption Technologies

Liquid chemical absorption technologies are mostly identical in function, with an absorber utilizing a gas-liquid contactor for absorption and a separate tank with either higher temperature or lower pressure for desorption. These technologies are currently the most widely used in point source carbon capture, with amine sorbents making up the majority of plants. But other liquid chemical carbon capture technologies are now reaching maturity, some with advantageous properties when compared to amine sorbents.

2.1.1 Liquid Amine Technologies

Liquid amine sorbents are chemical sorbents that often operate using a temperature swing, meaning the difference between absorption and desorption is caused by a temperature change. Advantages of amine technologies are the maturity of the technology and high capture rates even at low CO₂ weight percentages (wt.%). But downsides include high energy requirements, due to a strong chemical amine-CO₂ bond and the temperature swing, along with most types of amines forming airborne carcinogenic compounds when exposed to oxygen, resulting in additional cleaning requirements for the flue gas, increasing the total cost of the plant [8]. Furthermore, amines are corrosive[9] and often expensive, increasing the OPEX as constant sorbent makeup is needed. Some of these issues have been attempted mitigated, by designed various types of amine sorbents that can have properties

such as weaker amine-CO₂ bonds to lessen the energy consumption, less evaporation to lower the cleaning requirements or lower solvent degradation rates to lessen the replenishment rate. So while amine plants using amines such as monoethanolamine (MEA) have a theoretical minimum consumption of about 3 GJ/tonne CO₂ captured [10], plants with new types of amine sorbent have reached a theoretical consumption of only 2 GJ/tonne CO₂ [11], making them competitive with many emerging CC technologies. MEA amine technologies have a technology readiness level (TRL) of 9, according to EU's Horizon 2020 definition [12], whereas the new generation of amine processes with lower energy consumption, often named advanced amine systems, have a TRL of 8 [13].

2.1.2 Potassium Carbonate Technologies

Potassium carbonate has wide use cases in new carbon capture technologies, being used both as an absorbent and as a product when potassium hydroxide is used as absorbent. In point source capture, potassium carbonate is most often used as the absorbent, as potassium hydroxide has strong binding force to CO₂, requiring large amounts of energy and high temperatures to desorb again. In contrast, the weak binding energy of potassium carbonate, allows for low energy desorption of CO₂ [14], at the cost of a low rate of reaction, which means potassium carbonate systems tend to be larger than those of other carbon capture technologies. Furthermore, potassium carbonate can be considered corrosive to steel and some other common building materials, increasing the importance of material considerations when designing such a system. This can, however, mostly be negated by using corrosion inhibitors [15].

Due to the low rate of reaction, companies utilizing potassium carbonate technologies have to find ways to increase the capture rate in the absorber, in order to decrease the system size and make potassium carbonate viable as an absorbent, while also ensuring the absorbent does not destroy the system.

One such company is Capsol with their Capsol End-Of-Pipe system, which use pressure swing absorption to capture CO_2 using potassium carbonate. This system has internal heat generation, making it use only electricity and reportedly consume between 0.7 and 1.2 GJ/tonne CO_2 depending on the CO_2 wt.%[16], though this is electrical energy instead of heat energy. Their first large scale plant is currently being built in Sweden, which would bring their TRL to a 9 [17].

Another solution is proposed by the company Saipem called Bluenzyme, that use an enzyme named "Carbonic Anhydraze" to decompose the CO₂ molecules. This changes the the chemical equilibrium so that CO₂ can be absorbed by the potassium carbonate at low pressures and temperatures [18]. If this manages to achieve high capture rates at low pressure and temperatures, it could potentially become a leading capture technology in terms of energy efficiency. They have a

medium scale plant designed, bringing it to a TRL of 7, but nothing but test sites are yet to be built and larger scale systems are still being designed [13].

Lastly, some solutions use potassium hydroxide as a sorbent. While it is primarily used in direct air capture due to its high reaction rate with CO₂ at atmospheric conditions, it is also seeing use in experimental point source capture by the group ConcenCUS. ConcenCUS is funded by EU's Horizon 2020 Research and Innovation program and aims to negate the high temperature requirement of calcining potassium carbonate by using electrochemical desorption [19]. The first test of this technology in a relevant environment is currently being built, which will bring it to a TRL of 6.

2.1.3 Chilled Ammonia Technologies

Carbon capture using chilled ammonia as a sorbent is another emerging technology. It often relies on a temperature swing for absorption/desorption, by cooling the ammonia down to 2-10 °C before entering the absorber and then subsequently heating it, before it enters the desorber to release concentrated CO₂, much akin to amine processes, but with different temperature ranges. Chilled ammonia can allegedly reach higher efficiencies than classic amine technologies, as the chemical bond between ammonia and CO₂ is weaker than many amine-CO₂ bonds, with a specific heat duty of 2.46 GJ/tonne CO₂ [20] compared to approximately 3 GJ/tonne CO₂ for classic amines such as MEA [10]. But as mentioned earlier, new types of amines are being developed, some of which report specific heat duties below 2 GJ/tonne CO₂ [11], making chilled ammonia less efficient comparatively. But according to Baker Hughes, a company currently designing a chilled ammonia capture plant, chilled ammonia is very efficient at low mass percentages of CO₂ [21], something many new types of amines struggle with, potentially creating a niche for chilled ammonia to fill.

Other advantages for chilled ammonia include lower sorbent cost, potentially lower CAPEX due to lower temperatures and pressures, no toxic emissions and high CO_2 output pressure and concentration, reducing requirements for subsequent CO_2 cleaning and pressurisation/liquefaction [13]. Baker Hughes currently has the technology at a TRL of 7 [21].

2.2 Solid Adsorption Technologies

Solid adsorption technologies have been under development for several decades, but have suffered from low capture rates, low outputted CO₂ concentrations and fast sorbent degradation. But recently, advances in material sciences have led to materials with very advantageous properties, that may make solid adsorption a viable contender, often through materials such as zeolite 5A, zeolite 13X and metal-

organic framework (MOF), by having very selective and efficient adsorption, that can use a pressure swing for desorption [22]. Both zeolites and MOF's are microporous structures, that instead of reacting chemically with CO₂, selectively captures the CO₂ molecules perfectly within its structure. This means there is no chemical bond that has to be broken, potentially making desorption very efficient. Furthermore, as no toxic chemicals are involved it is non-toxic and the entire adsorption/desorption sequence could happen in a matter of minutes instead of hours, possibly allowing for smaller system sizes, as much less sorbent is needed [23][24].

No sources could be found on the efficiency of said systems, making the alleged "high efficiency" difficult to compare, but the new generation of this technology appear to be at a TRL of 5-6.

2.3 Cryogenic Technologies

Cryogenic technologies function by cooling or depressurising the flue gas till the CO₂ condenses or freezes, allowing for easy and highly selective separation. Cryogenic capture is known for being energy intensive, but saves energy on liquefaction and can achieve capture rates above 99%, several companies are therefore investigating this technology. Some companies, such as Chart Industries, are designing plants using only cryogenic capture. In Chart Industries Cryogenic Carbon Capture (CCC) system, the entire flue gas stream is cooled till the CO₂ condenses, allowing for separation, which they allege is energy efficient due to their heat integration [13].

But other companies, such as Air Liquide with their Cryocap system and Linde with their HISORP system, use a combination of carbon capture technologies to reduce the energy consumption. Their systems are designed to first capture a high percentage of the CO₂ using a pressure swing adsorption system using solid sorbents. The output concentration of this first step is expected to be 40-50% CO₂, which is then put into a cryogenic capture system [13]. Cryogenic systems often have high energy requirements, as the entire flue gas stream has to be cooled down, but by pre-filtering the CO₂, this energy requirement can be lowered while still maintaining a capture rate and output concentration above 95% and 99% respectively. Solid sorbents are ideal for this, as they are often energy effective and can capture high percentages of CO2, but have issues with outputting high concentrations of CO₂. Using a combination could, therefore, alleviate issues that the individual technologies face. As an alternative to solid sorbents, both companies have also proposed using the pre-combustion capture technology called oxy-fuel combustion as the first step, which will result in similarly high concentrations of CO_2 after combustion [25][13].

Cryogenic technologies are still under development, the systems begin designed by Linde and Air Liquide currently appear to be at a TRL of 6.

2.4 Membrane Technologies

Membrane technology is an emerging carbon capture field, where membranes that selectively allow CO₂ to pas through is used for capture. This technology requires high pressures to force the CO₂ through the membranes and membranes that are both very selective with letting CO₂ through and are capable of withstanding high pressures are still being developed. Despite this, systems utilizing the technology are already being developed, by companies such as CO2CRC, Honeywell and Linde, often utilizing many small membranes to prevent breakage[13].

While current membrane technologies mainly focus on cleaning acid gases, as many other carbon capture systems can struggle with this, it is also being designed for post-combustion carbon capture. Some companies, like Honeywell, are designing systems that solely rely on membranes to capture the CO₂, but as the membranes often require a flue gas pressure of about 200 bar to operate, membrane technology can easily face the same issue as cryogenic technologies does, which is having high energy requirements. Some companies, such as CO2CRC, therefore attempt to solve this in the same way as some companies designing cryogenic capture do, by adding a filter step before the membrane capture, to decrease the amount of gas that has to be pressurised [13].

This technology is still under development, but companies such as CO2CRC reports a TRL of 6 using a small scale system. They report that they can upscale with current technology, but larger membranes would be very beneficial to the scalability of the technology [13].

2.5 Pre-Combustion Technologies

The main pre-combustion technology currently being developed is oxy-fuel combustion, which consist of filtering oxygen out of atmospheric air before the combustion, so that the combustion is made in a highly oxygen-rich atmosphere. This means there is less nitrogen and other atmospheric gases in the flue gas, leading to high CO_2 concentrations. This flue gas can, therefore, either be cleaned and used directly, or be used in combination with other capture technologies that benefit from the higher CO_2 concentrations. On top of higher CO concentrations, oxy-fuel combustion also saves fuel in many processes, as there are less atmospheric gases to absorb the produced heat, ensuring more of the heat is used for its intended purpose. Oxy-fuel combustion systems are designed by companies such as Babcock & Wilcox and has a TRL of 9 [13].

2.6 Conclusion to State of the Art

To compare the outlined technologies for the purpose of selecting one for analysis, two key points have to be considered. First is how relevant the technology is for commercial use, that is how efficient it is, how mature it is and whether it has some other advantages compared to current technologies. The second point of consideration is how relevant further research would be to the advancement of the technology. If a technology has already been extensively researched with multiple publications, any further research may yield diminishing returns, technologies with few publications or other public information are therefore more desirable to focus on.

When only considering the first point, amine technology appear to be an obvious choice, while it does have drawbacks compared to other carbon capture technologies, such as having a corrosive solvent and carcinogenic fumes, the new generation of amine plants have high efficiencies, with energy consumptions of approximately 2 GJ/tonne CO₂, while also being a very mature technology. But due to the maturity of amine plants, research on these systems have been done many times before [26][27], lessening the relevance of subsequent reports on the subject.

Solid adsorption, cryogenic and membrane technologies all have high efficiencies and advantageous traits compared to existing technologies, while also having fewer existing reports on its function. But lower maturity means they are further from the commercial market and the systems may change drastically before becoming commercially available, which would make the analysis in this project irrelevant. The choice is, therefore, between potassium carbonate and chilled ammonia technologies. It is currently unclear whether chilled ammonia will stay a relevant technology, as its currently reported energy consumption of 2.46 GJ/tonne CO₂ is higher than that of the new advanced amine technologies, while having a lower TRL. Furthermore, while it does not have toxic emissions the sorbent, ammonia, is very toxic, increasing the hazard of leaks and other issues [28]. Potassium carbonate on the other hand has, as mentioned earlier, a projected power consumption between 0.7 and 1.2 GJ/tonne CO₂[16], albeit electrical energy, while also being non-toxic. While it does have other issues, such as low rate of reaction and potential corrosiveness, its high potential and low amount of publications make it ideal for the topic of this project, and is therefore chosen. Of the potassium carbonate technologies, Saipem's Bluenzyme and Capsol's End-Of-Pipe systems exist. Due to the lack of public information on the design of Saipem's Bluenzyme, making it difficult to recreate accurately, Capsol's hot potassium carbonate system called End-Of-Pipe (EOP) is chosen for further analysis. This system has high efficiency, no toxicity, high TRL and few publicly available reports on the system as a whole, making it highly relevant for a full system analysis.

Chapter 3

Problem Statement

The state of the art analysis in Section 2, gave an overview of upcoming carbon capture technologies and their current estimated relevance for this project. In that section, the technologies utilizing potassium carbonate as an absorbent are picked as the focus of this project, specifically the system called End-of-Pipe by Capsol. This technology was picked due to a high technology readiness level, alleged competitive efficiency and a lack of publicly available publications on its overall function. The aim of this project will, therefore, be to investigate various use cases for this system, with the aim of determining under what conditions it would excel. Based on this a problem statement was formed:

What is the performance of a hot potassium carbonate carbon capture system under varying operating conditions and under what conditions would the system perform the best.

To answer the problem statement, a numerical model of the End-of-Pipe system by CAPSOL will be made based on publicly available information. This model will be made in the modeling software Aspen Plus and using this model a sensitivity study will be made, to better understand various flue gases effect on the system. To supplement this, some system parameters will be explored to investigate how best to adjust the capture rate of the system to account for changing flue gases. Finally, the system's energy efficiency will be compared to that of a similar system, to determine what flue gas compositions this system would perform the best in, when compared to a similar system.

Chapter 4

Model Setup

In this chapter the chosen system will be described, in order to then set up a numerical model of said system. The description will be based on the patent filed by CAPSOL [29] and the report "Heat Integration and Optimization of Post-Combustion Hot Potassium Carbonate Carbon Capture" by M. B. Jeppesen [30], which is also the basis of the model used in this project.

4.1 System Overview

The Hot Potassium Carbonate (HPC) system utilizes a chemical reaction between potassium carbonate and carbon dioxide at high pressure, to separate CO_2 from the flue gas. the reaction is an ionic reaction as the potassium carbonate is dissolved in water, but is here written with whole compounds for clarity. The reaction can be seen in Equation 4.1. [31]

$$K_2CO_3(aq) + CO_2(aq) + H_2O(1) \leftrightarrow 2 \text{ KHCO}_3(aq)$$
 (4.1)

The chemical equilibrium of the equation can be controlled either by temperature or the concentration of CO₂ in the HPC solvent, consisting mainly of water and dissolved K₂CO₃. Pressure swing absorption functions by varying the pressure, as higher pressure will increase the solubility of CO₂ in the solvent, increasing the concentration of dissolved CO₂. This affects the absorbent reaction equilibrium, allowing for CO₂ absorption. Likewise, lowering the pressure will decrease the solubility of CO₂, decreasing the concentration and allowing for CO₂ desorption. Using a pressure swing can be advantageous compared to temperature swing, as the enthalpy released by the desorption reaction is mainly released as heat. In a temperature swing system this energy is deposited on the low temperature side, due to the absorption reaction being exothermic, making it difficult to recover. Comparatively in a pressure swing system the column temperatures can be very similar, as it is mainly the pressure and not the temperature difference driving the

reaction, this means heat recovery is often simpler if at all necessary. This can reduce the total energy consumption of the system [31].

Below, an overview of the system can be seen in Figure 4.1, with numbering used in the following paragraph to describe the system. The overall system setup is very similar to other liquid chemical absorption technologies, like liquid amine systems. But HPC systems, as mentioned previously, utilize a pressure swing instead of a temperature swing and in CAPSOLS EOP technology, which is the basis of this project, the heat production is integrated through the so-called "flash boxes", which electrify the systems heat production, and will be explained later in Section 4.1.1. These flash boxes are, however, not exclusive to HPC technology and could also be use for other carbon capture technologies [30].

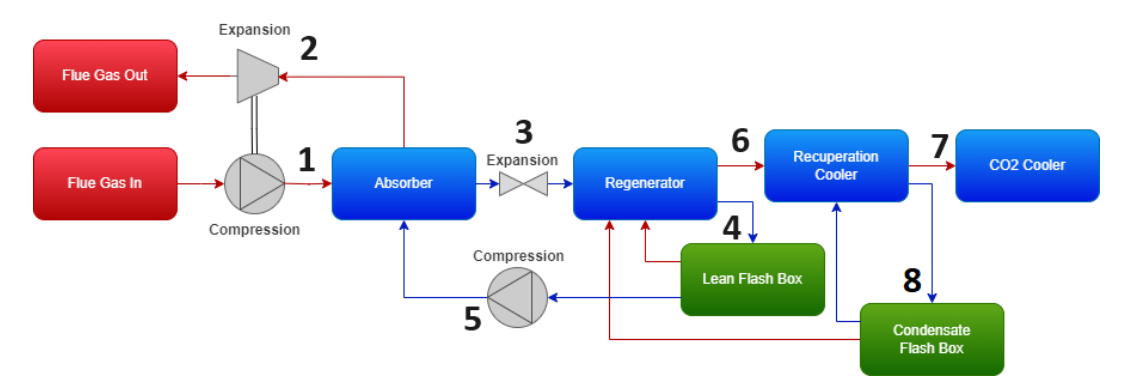


Figure 4.1: Flowchart of HPC process with flash boxes for integrated heating, based on figure from [30]. Numbers designate transitional areas between components.

As can be seen, the rich flue gas is pressurized (point 1 on Figure 4.1) and enters the absorber, where the CO_2 is filtered by a solvent, after which the now lean flue gas is heated using excess heat from the flue gas compression, and expanded through a turbine to recover energy (2). After the absorber, the solvent, now rich in CO_2 , is decompressed (3) and enters the regenerator, where the low pressure causes the CO_2 to be desorbed. Then the now lean solvent flows into the flash box (4), where some of its heat, along with external power, is used to produce steam to supply heat to the regenerator, to make up for heat losses in the system. After the flash box, the remaining lean solvent is recompressed and lead back into the absorber to repeat the loop (5). After the CO_2 is desorbed in the regenerator, the resulting gas stream contains mainly water vapor. To increase the CO_2 concentration of the gas stream and recoup some of this water vapor, the stream is cooled in the recuperation cooler (6) and CO_2 cooler (7) and the condensate from the recuperation cooler is used to run a secondary flash box, that also feeds steam to the regenerator (8).

4.1.1 Flash Boxes

The heat generation in the system is, as mentioned, mainly from the so-called "flash boxes", which are an integrated heating solution seemingly named by CAPSOL [17]. A flash box's main operation is identical to a standard mechanical vapor recompression (MVR) unit. A standard MVR unit consists of a separating tank (or flash drum), in which liquid close to its boiling point will enter and partly evaporate with no additional energy added. This is followed by a compressor that recompresses the produced steam, so it can be used for heating. The difference between an MVR system and a flash box system, is that a reduction valve is added before the separation tank, allowing for a compressor to lower the pressure in the tank further. By operating the separation tank at reduced pressure, the amount of steam produced increases, as decreasing the internal pressure decreases the boiling point.

A flash box is a heat recuperation technology, as the evaporation heat for the produced steam stems solely from the heat energy in the solvent. The increased steam production, therefore, results in increased heat recuperation, as each unit of steam produced yields a fixed amount of energy recuperated. But in return, the lower pressure in the separation tank results in a higher pressure difference over the compressor, leading to a higher power consumption per unit of steam and decreasing the coefficient of performance (COP). The advantage of flash boxes when compared to standard MVR systems, is increased steam production as well as higher resulting steam temperatures. This allows for all heat in the system to be generated by these mechanisms.

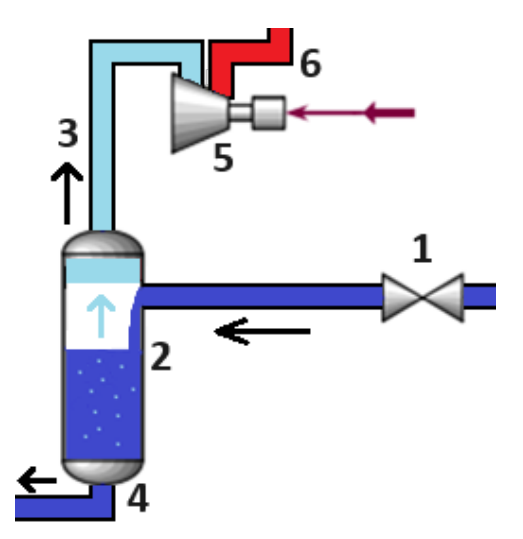


Figure 4.2: Figure displaying layout and function of a flash box.

A figure of a flash box system can be seen above in Figure 4.2, with solid blue

representing liquid, light blue low pressure steam and red high pressure steam. On the figure the reduction valve is denoted 1, separation tank denoted 2, low pressure steam stream denoted 3, leftover solvent leaving flash box denoted 4, compressor denoted 5 and high pressure/temperature steam leaving flash box denoted 6.

4.1.2 Absorber

The absorber consists of a packed column using vertical cross flow, with solvent entering at the top of the column and flue gas entering at the bottom. The packing ensures large surface area between the flue gas and solvent, which reduces the necessary size of the column and causes the flue gas and solvent to be approximately equal temperatures. The absorber is at a pressure of approximately 5 bars, which means both the solvent and flue gas has to be pressurized previous to entering it. The pressurization is, as mentioned earlier, necessary for the absorption of CO_2 into the solvent. The main chemical reaction occurring in the absorber is, as mentioned at the beginning of Section 4.1, $K_2CO_3 + CO_2 + H_2O \rightleftharpoons 2$ KHCO₃ and due to the high pressure in the absorber, the point of chemical equilibrium is towards the right side of the equation, making it absorb the CO_2 . This is an exothermic reaction and in this case occurs at approximately 90 °C.

Due to the large surface area between solvent and flue gas, the temperatures of the fluids are approximately equal at a set location, but will vary along the height of the column, as heat is transferred between streams. The exception to this is at the end of the column where the fluid with lowest heat capacity rate, that is heat capacity per second, enters, as this stream is unable to completely cool/heat the other fluid stream to its own initial temperature. In a liquid-gas column, the lowest heat capacity rate stream will often be the gas stream, which means in the end of the column where the gas stream enters, a larger temperature difference between the incoming and outgoing streams can be observed than the opposite end, where the streams will likely be very close in temperature.

4.1.3 Regenerator

The regenerator is similar to the absorber, in it being a packed column of approximately equal size and temperature, with the same rules for temperature distribution. But the internal pressure in the regenerator is approximately 1 bar, which reverses the reaction in the absorber, now releasing the CO₂ and regenerating the solvent. This reaction is, of course, endothermic, which means heat is required to sustain the reaction. The regenerator is therefore where heat is added to the system to make up for heat losses. This is done by two means, one is steam from the flash boxes and the other is steam from a reboiler attached to the regenerator. This reboiler is driven solely using heat from the rich flue gas after it is pressurized, but before it enters the absorber (see point 1 on Figure 4.1). This cooling is

advantageous, as the absorber temperature should be kept below a certain level, as the equilibrium of the absorbent reaction changes with increasing temperatures, reducing the capture rate and rate of reaction if temperatures are too high. Cooling the flue gas stream by heating the reboiler is also advantageous, as it increases the temperature in the regenerator, where the rate of reaction goes up with temperature due to it being an endothermic reaction.

Due to the higher temperature and amount of steam in the regenerator, the outputted gas stream is, as mentioned earlier, mainly water vapor by weight. As the output stream is desired to be approximately 95% CO₂ by weight, the recuperation cooler and CO₂ cooler are added.

4.1.4 Recuperation Cooler

The recuperation cooler is a condensation tank, solely utilizing water from the condensate flash box and CO₂ cooler to cool the CO₂ gas stream, in order to condensate part of the water vapor in the stream. This works, as the water from the condensate flash box have a lowered temperature, due to some of its heat energy having been used to produce steam in the flash box, and the water from the CO₂ cooler have been cooled using external cooling to force further condensation.

The heat equation of the recuperation cooler is:

$$0 = \dot{m}_{hot} \cdot (T_{hot} - T_{combined}) \cdot c_{p,hot} - \dot{m}_{cold} \cdot (T_{combined} - T_{cold}) \cdot c_{p,cold} + \dot{m}_{cond} \cdot \Delta H_{vap@T}$$

$$(4.2)$$

Which simply describes the energy balance between the incoming gas stream (hot) and incoming liquid stream (cold) when mixed and reached thermal equilibrium (combined), with the last term describing the energy added from steam condensation.

4.1.5 **CO2 Cooler**

Once the CO_2 stream exits the recuperation cooler, external cooling is required to cool the stream sufficiently to condense enough water vapor to reach a CO_2 concentration of 95%. This cooling can be achieved using either utility or by producing district heating, if the temperatures are sufficient. The amount of cooling required depends on the vapor content of the CO_2 stream once it exists the recuperation cooler.

The heat equation of the CO_2 cooler is similar to that of the recuperation cooler, except it is cooled by an external source.

$$0 = \dot{m}_{hot} \cdot (T_{hot} - T_{combined}) \cdot c_{p,hot} - Q_{cooling} + \dot{m}_{cond} \cdot \Delta H_{vap@T}$$
 (4.3)

Which similarly to Equation 4.1.4 states the energy balance, although now between a gas stream and an unknown cooling stream (cooling).

4.2. Chemistry

4.2 Chemistry

The overall reaction mentioned in Equation 4.1, can be separated into five reactions, represented by the following equations, of which the first two are dissociation reactions, as they are dissolved in water:

$$K_2CO_3 \rightarrow 2K^+ + CO_3^{2-}$$
 (4.4)

$$KHCO_3 \rightarrow K^+ + HCO_3^- \tag{4.5}$$

And the other three are equilibrium equations that cause the capture of CO₂.

$$2\,H_2O \leftrightarrow OH^- + H_3O^+ \tag{4.6}$$

$$CO_2 + OH^- \leftrightarrow HCO_3^-$$
 (4.7)

$$CO_3^{2-} + H_3O^+ \leftrightarrow HCO_3^- + H_2O$$
 (4.8)

As seen by these reactions, the sorbent does not absorb the CO_2 directly, but is dissociated into K^+ and CO_3^{2-} in Reaction 4.4. Here the CO_3^{2-} is used to react with the H_3O^+ produced in the autoionization of water in Reaction 4.6, to reduce the concentration of H_3O^+ . This is important as the other product of Reaction 4.6 is OH^- , which is used in Reaction 4.7 to react with, and thereby capture, CO_2 in the form of HCO_3^- . While this capture reaction would happen on its own with no sorbent added, Reaction 4.6 would quickly reach equilibrium due to the H_3O^+ concentration and the overall capture would be minimal, the absorbent is therefore added as it reacts with, and thereby lowers the concentration of, H_3O^+ in the solution, allowing for more OH^- to be produced and consequently react with CO_2 to capture it.

What reaction limits the overall rate of reaction depends on the pH of the solution, but it is generally agreed upon that above a pH of 8, it is reaction 4.7, meaning Reaction 4.6 and 4.8 are significantly faster [32]. As these reactions are often faster than the rate of CO₂ mass transfer into the solvent, their rates of reaction are often considered negligible and, therefore, set as equilibrium equations. But due to the lower reaction rate of Reaction 4.7, it it not necessarily faster than the mass transfer of CO₂ into the solvent, and therefore its kinetics cannot be ignored [33].

Reaction 4.6 and 4.8 can be expressed through an equilibrium reaction, as seen in Equation 4.9.

$$ln K_{eq} = A + \frac{B}{T} + C ln T + DT$$
(4.9)

In which K_{eq} is the equilibrium constant, T is the temperature in Kelvin and A, B, C, D are reaction specific constants.

For reactions requiring kinetics to be simulated, the rate based reaction has to be defined. The rate of reaction can be calculated using Equation 4.10, in which r is the reaction rate, k_1 and k_{-1} the rate coefficients, [HCO₃ $^-$], [CO₂] and [OH $^-$] the molar concentrations and the exponents a, b and c are the partial reactions orders.

$$r = k_1[\text{CO}_2]^a[\text{OH}^-]^b - k_{-1}[\text{HCO}_3^-]^c$$
 (4.10)

The rate coefficients *k* are found experimentally, but vary depending on temperature. The correlation between rate coefficient and temperature can be approximated using the modified Arrhenius Equation, as seen in Equation 4.11 [34].

$$k = A_{pre} T^n e^{\frac{-E}{RT}} (4.11)$$

In which A_{pre} is the pre-exponential factor, E is the reaction's molar activation energy, R is the ideal gas constant, T is temperature, and n is a fit constant, to compensate for non-ideal behavior. This can be further expanded by adding a reference temperature, which compensates for a difference between the temperature in the simulation and the temperature at which the expression was found.

$$k = A_{pre} \left(\frac{T}{T_0}\right)^n e^{\left(\frac{-E}{R}\right)\left[\frac{1}{T} - \frac{1}{T_0}\right]}$$

$$\tag{4.12}$$

Where T_0 is the reference temperature [34].

4.3 Model setup in Aspen Plus

In this section, a steady-state, full system, Aspen model of the CAPSOL carbon capture plant will be designed. The model will be set up in Aspen Plus V12.1 and will be built to explore the behavior and functions of the system, with a focus on comparing various use cases of the system, to discover what scenarios this specific system would be optimal in, potentially making it easier to compare the usefulness of various carbon capture systems in specific circumstances.

4.3.1 Basis of the Model

As the model is based on a real system, it will have approximately the same layout as shown in Figure 4.1 and the reactions shown in Section 4.2. The model was first attempted made in Aspen Hysys V12.1, but was due to difficulties with implementing the solvent instead made in Aspen Plus V12.1. The initial values of the model were mainly from the report by M.B. Jeppesen (2024) [30], both for system sizing and initial mass flows, as the values of that report are based on the values

of CAPSOL's patent on the system. But that report used the integrated "acid-gas" package in Hysys V14, which automatically implements chemical reactions, mass flow ratios and fluid properties for the potassium carbonate solvent, as well as recommend solvers and what thermodynamic models to use. This package does not exist in neither Aspen Hysys V12.1 or Aspen Plus V12.1, nor does all the solvers used, which meant these values and new solvers had to be found and implemented manually. As these values govern how accurate the model will be compared to real life systems, implementing correct values and approximations is paramount for the model to produce useful data.

4.3.2 Model Chemistry

To model the chemical reactions in the system, an electrolyte-NRTL (eNRTL) thermodynamic model is used, as it is proven to be one of the most accurate models for liquid-liquid and gas-liquid reactions [35] and is especially applicable for CO₂ capture as it is good at correcting non-ideal behavior [36]. The eNRTL model functions by calculating close range molecular interactions using a non-random two liquid (NRTL) model and long range inter-molecular forces using the Pitzer–Debye–Hückel formula [36]. To calculate gas properties for the vapor phase, a Soave–Redlich–Kwong equation of state is used [37].

In this project, the reactions will be fully rate based to investigate how accurate a fully rate based model is, as a fully rate-based model is often necessary for the creation of dynamic models.

To accomplish this six kinetic equations are necessary, two for each equilibrium model. The forwards reaction for Reaction 4.7 can be found in an article by Pinsent et al. [38], which is proved in an article by Savage et al. [32] to be applicable for temperatures up to $110\,^{\circ}$ C, and the backwards reaction can be found in an article by Borhani et al. [33].

The reaction rates for Reaction 4.6 and 4.8 were not able to be found. This is likely due to both reactions being ion exchange reactions, which tend to have rates of reaction magnitudes higher than most other reactions, causing them to rarely be the limiting reaction. This is, of course, also true in this case as Reaction 4.7 is the limiting reaction [33].

To approximate Reaction 4.6 and 4.8 a forward rate of reaction will be manufactured. As the reactions are near instantaneous and limited by the rate of reaction of Reaction 4.7, the rates of reaction for Reaction 4.6 and 4.8 simply need to be sufficiently higher, to ensure Reaction 4.7 remains the limiting reaction. Once a sufficiently high forward rate of reaction have been found, the backwards rate of reaction can be found by calculating the ratio between the forward and backwards rate of reaction, using the equilibrium equation. The activation energies of the reactions can then be approximated based on the difference in enthalpy between

reactants and products, assuming the entropy is negligible, this is shown below.

Starting with the Arrhenius equation from Equation 4.11, with a temperature exponent b equal to zero, as shown in Equation 4.13.

$$k = A_{pre} e^{\frac{-E}{RT}} \tag{4.13}$$

Where k is the rate coefficient, A_{pre} is the pre-exponential factor, E is the activation energy, R is the universal gas constant and T is the temperature.

Then using an equilibrium equation, as seen in Equation 4.9, the equilibrium constant is calculated at a set temperature and used in Equation 4.14 to calculate the rate coefficient k_2 of the backwards reaction, by knowing the equilibrium constant K_{eq} and forward rate coefficient k_1 .

$$K_{eq} = \frac{k_1}{k_2} \tag{4.14}$$

Then, assuming there is no entropy, the activation energy of the backwards reaction E_2 can be found, by knowing the activation energy of the forwards reaction E_1 and the change in enthalpy between reactants and products ΔH , as seen in Equation 4.15 below. If no forwards activation energy is known, it too can be approximated by adding the enthalpy of its reactants.

$$E_2 = \Delta H + E_1 \tag{4.15}$$

And then Equation 4.13 can be set up for the backwards equation and solved for the pre-exponential factor A.

Finally, a test can be done to calculate whether the results match the equilibrium equation, by checking whether the results of the kinetic reaction and the equilibrium reactions equal each other. This is done by setting up a forwards and backwards equation for the rate of reaction, using Equation 4.16, and inputting molar reactant and product concentrations that, according to the equilibrium equation, should be at equilibrium. Then the forwards and backwards rate of reaction should equal.

$$r = k [MolA]^a [MolB]^b (4.16)$$

Here, *r* is the rate of reaction, *k* is the rate coefficient, MolA and MolB are the molar concentrations of the reactants and a and b are the partial reaction orders. The equilibrium equations used for these calculations are from an article by Edwards et al. (1978) [39]. Below two tables containing the values used in this project can be found.

Reaction	A	В	С	D	Temperature range
Reaction 4.6	132.899	-13 445.90	-22.477	0	0 - 225 °C
Reaction 4.8	216.049	-12 431.70	-35.4819	0	0 - 225 °C

Table 4.1: Equilibrium equations

Reaction	A _{pre}	E (kJ/mol)	Temperature range
Reaction 4.6 Forwards	$3.8 \cdot 10^{17}$	74.475	-
Reaction 4.6 Backwards	$1 \cdot 10^{30}$	144.117	-
Reaction 4.7 Forwards	$4.315 \cdot 10^{13}$	55.434	0 - 110 °C
Reaction 4.7 Backwards	$2.38 \cdot 10^{17}$	123.223	0 - 110 °C
Reaction 4.8 Forwards	$3.02 \cdot 10^{14}$	41.20	_
Reaction 4.8 Backwards	$2.26 \cdot 10^{26}$	62.91	-

Table 4.2: Rate based Arrhenius equations

4.3.3 Aspen model

Below in Figure 4.3 the Aspen V12.1 model can be seen. The layout is mostly identical to the flowchart shown in Figure 4.1 in Section 4.1. The changes made are mostly miscellaneous additions, such as the makeup stream, water recuperator and overflow return, which are mainly practical additions to aid the system's function.

To elaborate, the makeup stream, located between the lean flash box and absorber, adds water and absorbent as needed, ensuring a constant solvent flow and concentration. The water recuperator, placed on the flue gas stream after the absorber, reduces the amount of needed makeup water and allows for more expansion of the flue gas stream without condensation. The overflow recirculation, placed between the recuperation cooler and the condensate flash box, controls the amount of water entering the condensate flash box, to ensure water does not accumulate in the condensate flash box and recuperation cooler loop.

It is also worth noting, that the flue gas "compression" step is separated into two compressors, this is to better simulate the mechanical connection between the flue gas expander and compressor, as all energy recovered in the "Flue gas expansion" step is, in this project, used to power part of the compression. In a real system it could, however, be beneficial to separate the flue gas compressor into two and adding an intercooler between them, as this could increase the system efficiency by several percentage points at the cost of lower heat production in the system. The lowered heat production would have to be compensated for by lowering the flash box pressures, but as the flash boxes are energy recuperation systems, unlike compressors, this will likely still net energy savings. But, as the goal of this project is to focus on the effects of various flue gas compositions on the system, as well as the flash boxes effect on the system as a whole, changes to the system layout

will not be made to other parts of the system and the effects of an intercooler will, therefore, not be investigated further in this project.

21

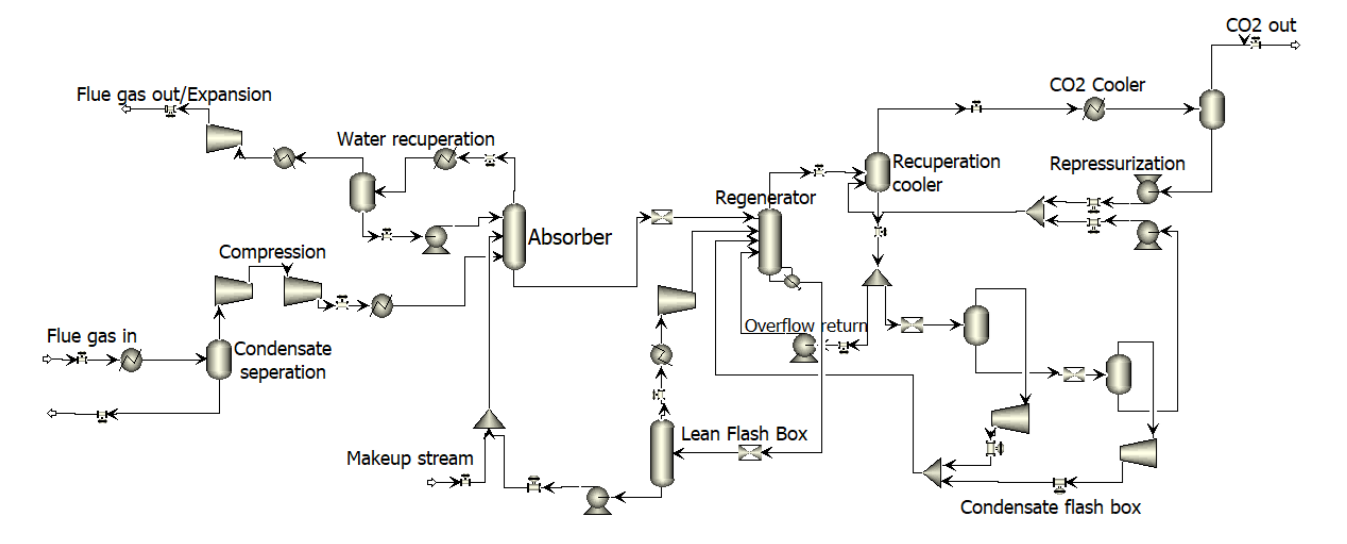


Figure 4.3: Overview of the model in Aspen Plus V12.1, with text designating various parts of the system

	System Specifications				
Absorber height	25 meters	Absorber width	10 meters		
Regenerator height	25 meters	Regenerator width	10 meters		
Lean flash box height	10 meters	Lean flash box width	10 meters		
Absorber pressure bot	5 bar	Regenerator pressure bot	1.31 bar		
Lean flash box pressure	0.62 bar	Cond. flash box high pressure	0.424 bar		
Cond. flash box low pressure	0.374 bar	Flow into condensate flash box	500 kg/s		
Regenerator reboiler duty	38 MJ/s	Capture percentage wt.%	90%		
Flue gas in	235.8 kg/s	flue gas CO ₂ conc. wt.%	22.65%		
Lean absorbent flow rate	2400 kg/s	Lean K ₂ CO ₃ conc. wt.%	25%		

Table 4.3: Overview of the specifications used for the initial system

4.4 Validation of Model

To validate the accuracy of the model, experimental data on the partial CO_2 pressures and mole loading of the absorbent at various temperatures by Tosh et al. [40] is used. To ease the comparison, a report by Anusha Kothandaraman [41] is used, as the experimental results by Tosh et al. are in this work summarized, converted from psi into atmospheric partial pressure and used to adapt a vapor-liquid equilibrium model that fits the experimental data. The results from this vapor-liquid

22

equilibrium model will be used to validate the model of this project for a clearer comparison.

Below in Figure 4.4 the experimental data from Tosh et al. and the model data of Kothandaraman is shown, with the horizontal axis being the mole loading of the absorbent, which is moles of absorbent saturated with CO₂ divided by total moles of absorbent, and the vertical axis being the partial pressure of CO₂ in atmospheres of pressure (atm). The data points are sorted by temperature, each interval being differentiated by change in color and marker shape.

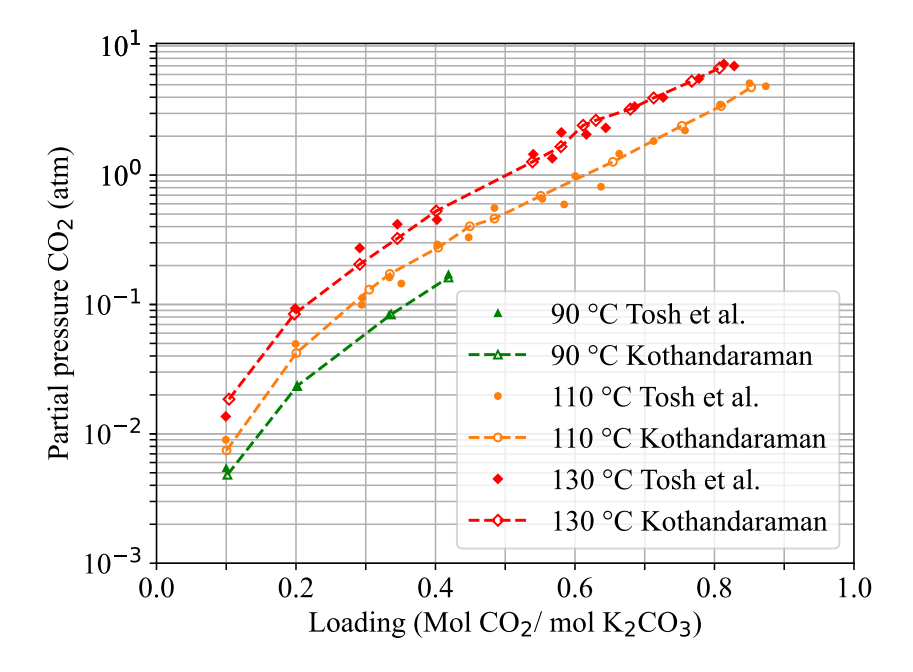


Figure 4.4: Figure showing the experimental results of Tosh et al. compared to the simulated results of Kothandaraman, data taken from [41]

As can be seen, the model by Koshandaraman is very well fitted to the experimental data, and can, therefore, be used with decent accuracy to represent the experimental data in a comparison between this projects model and the experimental data of Tosh et al.

In Figure 4.5 the results of this projects model and the model of Anusha Kothandaraman can be seen. The axes are the same units as the previous figure, with the horizontal axis being the mole loading and vertical axis being partial CO₂ pressure. The data points marked "Model" in the legend are results from this projects model.

It can be seen in the figure, that at 90 °C and 110 °C the model of this project diverges with 14% to 17% from the model of Kothandaraman, while the slopes and ratios between different temperature levels remain approximately equal. While loading for a set partial CO₂ pressure is of import, the most important part is the ratios between various temperature levels being correct. As these ratios are very

23

similar to the results of Kothandaraman, a divergenge of approximately 15% is deemed acceptable for the purposes of this project.

It is, however, important to note that the highest temperature for each model is not equal, this is due to the model of this project not converging at temperatures above 128 °C in the absorber, which is where the results have been measured. As can be seen in Figure 4.5, the partial CO_2 from this project's model at 125 °C are higher than that of Kothandaraman's model at 130 °C, and appear higher than they should be, when compared to the results at 90 °C and 110 °C. This may be caused by the model diverging from expected results at higher temperatures, possibly due to the rate-based reactions being too far from their reference temperatures.

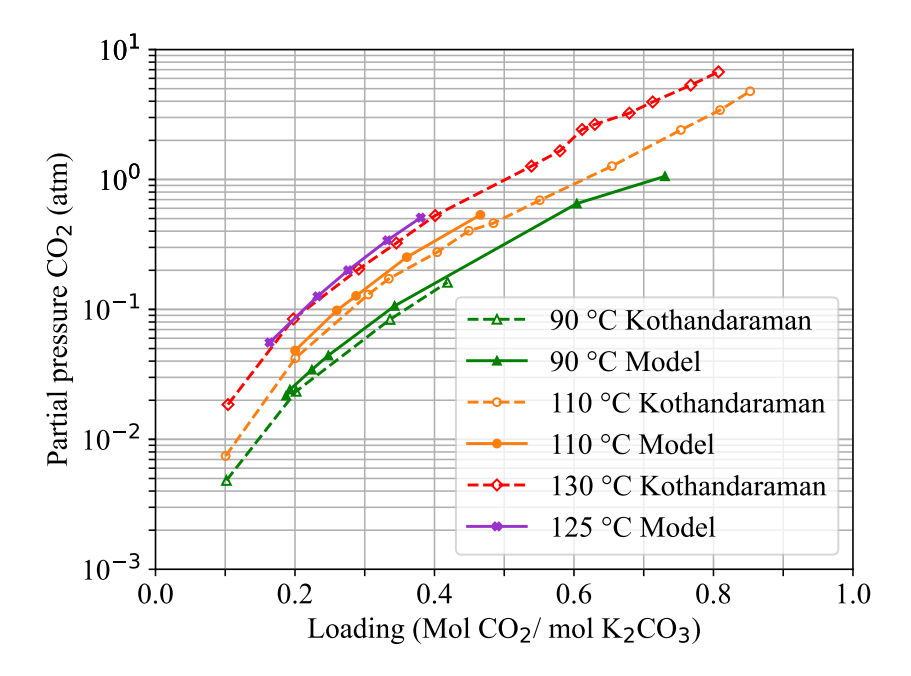


Figure 4.5: Figure showing the results of this projects model, taken in the absorber, compared to the model of Kothandaraman

To more accurately assess the boundaries of the model and whether it is viable to remain within them for the purposes of this project, the maximum temperature of the model is found. This is done by measuring the partial CO_2 pressure in the model every 5 °C from 90 °C to 110 °C at a constant absorbent loading. This temperature range is chosen as it is the range in which the model is validated. The measurements are used to predict the expected partial pressure at higher temperatures than 110 °C, by fitting a function to the five known points, the results of this can be seen below in Figure 4.6. In this figure, the horizontal axis is the temperate in celsius and the vertical axis is the partial CO_2 pressure. The results have a constant absorbent loading of 30% and has the points within the validated

4.4. Validation of Model

24

range shown as blue, the points outside this range shown as orange and the fitted function shown as a blue dashed line.

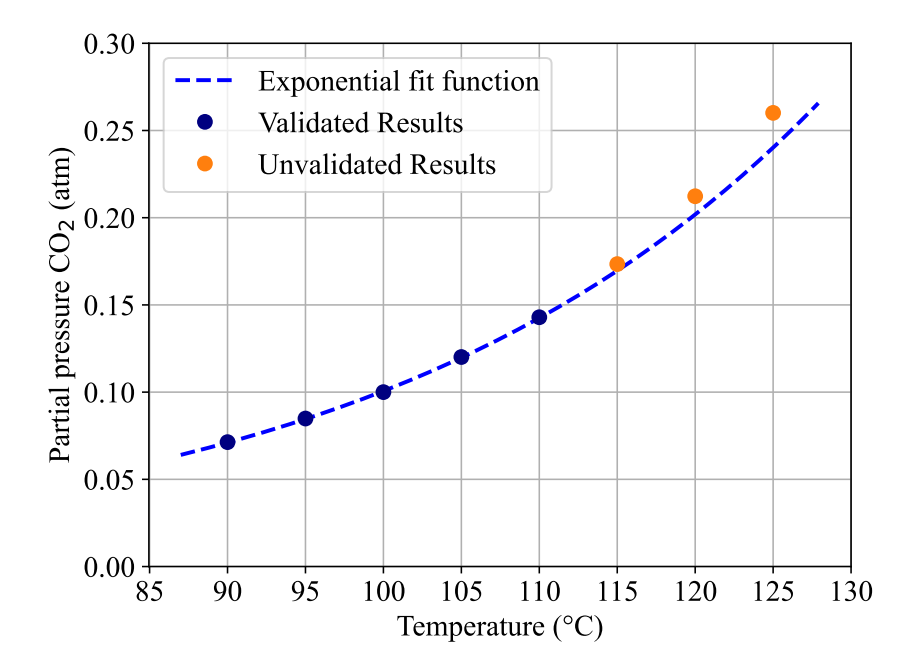


Figure 4.6: Figure showing the measured partial CO₂ pressures at various temperatures and constant absorbent loading, with a fitted function to estimate the expected partial pressures at temperatures beyond what is validated.

Based on the data from Figure 4.6, it can be calculated that the partial CO₂ pressure at 115 °C is 2.2% higher than expected, at 120 °C 5% higher than expected, and at 125 °C 8.3% higher than expected. To remain within a 5% uncertainty, in order to maintain the ratio between temperature and partial pressure at a set loading, the model's maximum temperature is set to 120 °C at locations where reactions are simulated, which is the absorber, regenerator and lean flash box. As the temperatures at these locations are unlikely to exceed 115 °C, it is viable to remain within the boundary of 120 °C, and the model is therefore acceptable for this project.

Chapter 5

Results and discussion

In this chapter the results of the model will be presented, analyzed and discussed, in order to answer the question asked in the problem statement.

5.1 Utility Requirements

In this section the potential utility requirements of the system will be explored, to investigate what additional requirements the systems may have. This is especially important for this system, as a potential benefit of an electrified system with integrated heating is its low infrastructure requirements, which could increase its viability in areas that are remote, therefore having increased utility costs, or areas that are completely lacking in the necessary infrastructure, resulting in new infrastructure having to be built to facilitate a carbon capture system.

To analyse the heat consumption, a pinch point analysis of the system is made, and can be seen below in Figure 5.1. On this figure, the required cooling is displayed with a blue line and the heating as an orange line, with the horizontal axis being the enthalpy per kg CO₂ captured and the vertical axis the temperature at which the heating or cooling is required. The pinch point is set to be 10 °C.

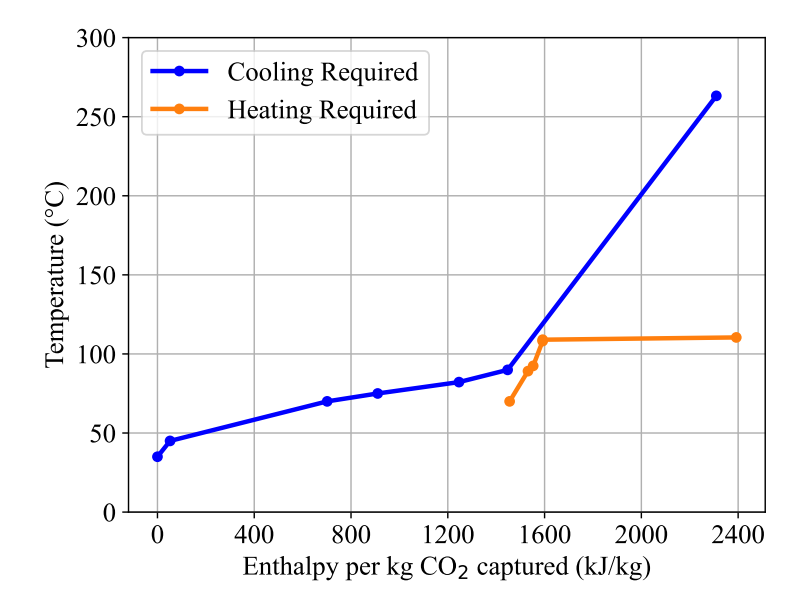


Figure 5.1: Pinch point analysis of the system, with a blue line designated required cooling and orange line designating required heating.

On Figure 5.1, it can be seen that while some heat exchange can take place, both hot and cold utility is still required with the current system configuration. The required hot utility is about 80 kJ/kg CO₂ at over 110 °C and is needed for the regenerator reboiler. The required cold utility is about 1450 kJ/kg CO₂ of cooling, and is needed to cool streams in the temperature range of 35 °C to 90 °C. This cooling is used to cool the flue gas stream and CO₂ stream at various places to, for example, reduce the flue gas temperature previous to it entering the absorber or to remove water vapors previous to the flue gas being compressed or expanded. For the CO₂ stream, cooling is used to dry the gas stream, to ensure it is outputted with at least 95% CO₂ in mass.

The heat balance in the system can, however, quite easily be manipulated. The heating requirement can, for example, be changed by varying the reboiler duty and then changing the flash box pressure to compensate, although this would likely also change the power consumption of the system, as the flash box depends on a compressor to upscale the recuperated heat energy. Alternatively the cooling could be changed by, for example, changing the absorber pressure, this would change how much the flue gas is compressed and, therefore, change the high temperature cooling requirements. But this would, of course, also change the power consumption along with the rate of reaction in the absorber, as higher pressures increase the partial pressure of CO₂, thus facilitating faster rates of reaction and potentially better capture rates.

This will be demonstrated in order to remove the heating requirement. The result of this adjustment can be seen below in a new pinch point analysis in Fig-

ure 5.2. The adjustment mainly consist of reducing the heating requirement, by reducing the regenerator reboiler's heating duty by about 52 kJ/kg CO₂ and compensating for the lower heat production, by lowering the flash box pressure. As the flash box is an energy recuperation system, this also reduces the overall cooling requirement of the system and the increased power consumption from the lowered flash box pressure is, in this case, completely offset by increasing the heat exchanged at the flue gas heater, to increase power recuperation in the flue gas expander. This works as the flue gas heater is the last heat exchanger before the flue gas expander, and increasing its heating duty increases the flue gas' temperature, and thereby volume, previously to it being expanded.

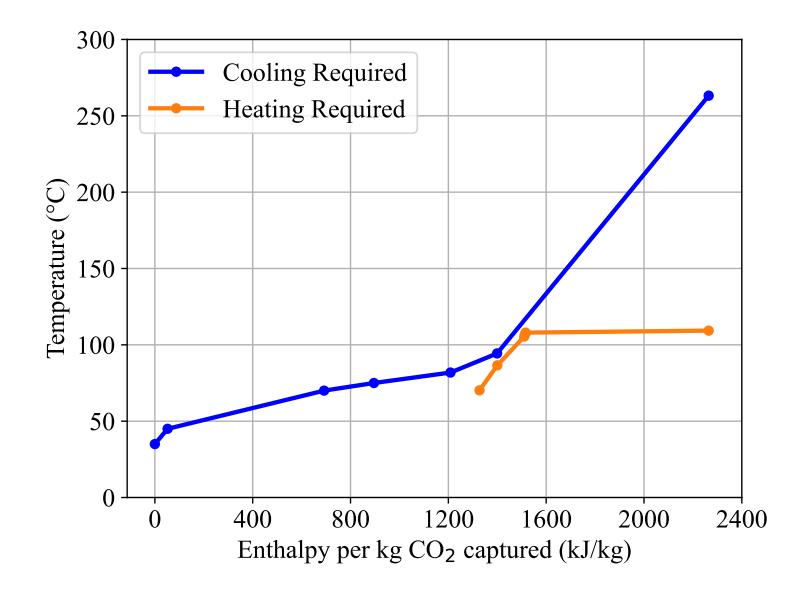


Figure 5.2: Pinch point analysis of the system, with a blue line designated required cooling and orange line designating required heating.

To explain what exactly can be seen on this figure, the high temperature cooling requirements are from the post compression flue gas cooling, to reduce the flue gas temperature before it enters the absorber. The lower temperature cooling requirements (below 90 $^{\circ}$ C), are mainly from the condensation of water vapor in the flue gas and CO_2 streams as mentioned previously. The heating requirements largely stem from the reboiler in the regenerator, the remainder being the flue gas heater pre-expansion, to increase the energy recuperation from the expander, and the heater attached to the steam output of the lean flash box, to increase the heat recuperation of the system.

As can be seen on the figure (Figure 5.2), all heating requirements can now be covered by the cooling requirements, but all the lower temperature cooling, from 35 °C to 90 °C, requires external cooling, this amounts to approximately 1330 kJ/kg

CO₂. In this interval, approximately 87.5% of the cooling energy requirement is between 50 °C and 90 °C and approximately 96.5% between 40 °C and 90 °C. This means the system would be a great candidate for district heating production, particularly for 4th generation district heating, as 4th generation district heating operates between 30 °C and 70 °C [42]. This temperature interval means the system could convert almost all excess heat to district heating without requiring a heat pump, which would remove almost all cooling requirements. Alternatively, 3rd generation district heating could also be produced, but this would require a heat pump, but could still potentially reduce or completely remove the utility costs associated with cooling, if the district heating can be sold.

It does, however, also mean that for real world applications, access to costeffective cooling would be important to the construction of this plant, as a relatively large amount of cooling is required.

5.2 Sensitivity Analysis

A carbon capture system's capture efficiency tends to be affected by a number of external and internal variables, one such variable that tends to have a big effect these systems, is the composition of the incoming flue gas stream. This composition can, for example, affect the amount of make-up water needed, the rate of sorbent degradation due to impurities and, the focus of this section, the capture rate of the system. The flue gas parameter that affects the capture rate the most is the CO₂ concentration. This is because a decrease in CO₂ concentration of the flue gas, means the system either captures less CO₂ overall at approximately the same energy requirement, lessening it's energy efficiency, or the flue gas flow rate has to be increased to match the high concentration CO₂ flow, in which case more flue gas has to go through the system which increases the energy consumption.

The degree to which this affects various carbon capture systems is, however, not necessarily equal. This means a system can specialize in operating under certain conditions, by being more energy efficient than similar systems when scrubbing a flue gas with a certain CO_2 concentration.

In this section, the characteristics of the HPC carbon capture system with varying flue gas compositions will, therefore, be investigated, to compare to similar systems and discover potential trends.

5.2.1 Effects of Various Flue Gas Compositions on System Efficiency

While the flue gas composition can vary due to many reasons, the most influential reason is likely the source of the flue gas changing. Below, in Figure 5.3, the power consumption and cooling requirements can be seen from three of the highest CO₂ producing sources, which are coal power plants, natural gas power plants and

cement plants. The mass flow, initial temperature and initial pressure of all three flue gas streams are equal and the capture rate have been adjusted to 90% for all cases by varying the lean flash box pressure.

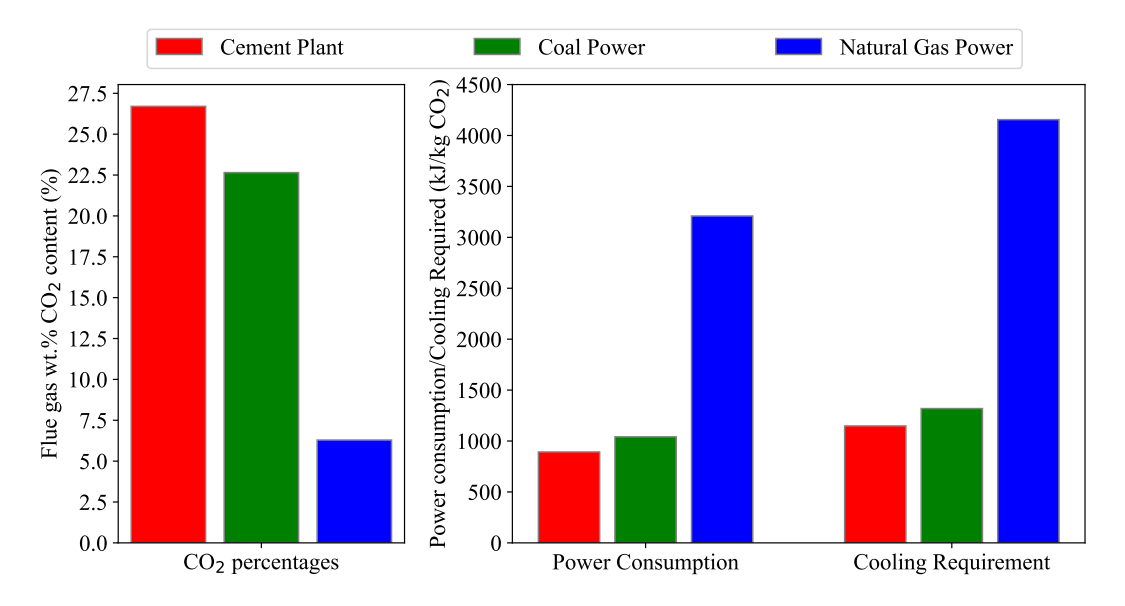


Figure 5.3: Comparison of power and cooling requirements per kg CO₂ captured for flue gases of various origins. With red bars (leftmost) being from a cement plant, the green bars (center) being from coal power, and the blue bars (rightmost) being from natural gas power.

As can be seen on the leftmost part of the figure, which displays the CO₂ percentages of the flue gases, there is a large variation in the CO₂ content of the three flue gasses. When comparing the CO₂ percentages with the power consumption and cooling requirements, shown on the right side of the figure, the aforementioned correlation between CO₂ concentration and efficiency can be seen, with lower CO₂ percentages leading to higher power consumption. It can also be seen that the cooling requirements follow the increase in power consumption fairly well. This is interesting, as the highest cooling requirements in the system, are cooling the rich flue gas after compression, which is only marginally affected by varying the CO₂ percentage, and drying the CO₂ stream after the regenerator, which could be reasoned would require less energy as the CO₂ mass flow is lower. But the reason for increased cooling requirements, is that the power increase is used to generate more heat, which increases the temperature in the regenerator and absorber, this increases the amount of water being evaporated, leading to the gas streams from both having much higher moisture contents, both of which then require more cooling to dry the streams. That also mean that this cooling is below 90 °C, where it is unusable for heat exchange with other parts of the system and, therefore, has to come solely from external cooling.

Below in Table 5.1 the flue gas compositions of the three streams can be seen, the coal flue gas is the same as used in the rest of the project and is similar to the coal power flue gas reported by other sources, such as Güleç et al. (2020) [43] and Schakel et al. (2018) [44].

Flue Gas	H ₂ O	O_2	N_2	CO_2	Temperature
Coal Power wt.%	7.5	5.5	64.35	22.65	70 °C
Coal Power mol%	12.25	5.05	67.56	15.14	70 °C
Cement Plant wt.% [45]	11.18	8.18	53.95	26.7	70 °C
Cement Plant mol% [45]	18.2	7.5	56.5	17.8	70 °C
Natural Gas Power wt.% [43]	5.55	13.68	74.5	6.29	70 °C
Natural Gas Power mol% [43]	8.67	12.09	75.2	4.04	70 °C

Table 5.1: Flue gas compositions used in Figure 5.3

To put the performance shown in Figure 5.3 into perspective, the performance of the HPC capture system is compared to that of an amine MEA capture system, by varying the CO₂ concentration of the coal power plant flue gas, measuring the power consumption, and comparing it to the energy consumption of a numerical model of an MEA system by Husebye et al. (2012) [46]. This can be seen below in Figure 5.4, in which the CO₂ concentration of the flue gas of both systems are varied with a constant capture rate of 90%. The capture rate of the HPC system was kept constant by adjusting the flash box pressures.

It is important to note, that the energy consumed by the HPC system is solely electrical power, whereas the energy for the MEA system is 90% heat energy, with the remaining 10% being electrical power. The magnitudes are, therefore, not directly comparable and instead the point of interest is their slope, to ascertain whether they are comparatively more efficient at certain CO₂ percentages. Furthermore, the CO₂ percentages are in mol% instead of wt.% unlike the rest of the project, as these are the units used by Husebye et al. [46]. The range in which theCO₂ concentration in the flue gas is varied here for the HPC system, is from 2.1 mol% to 18.5 mol%, in wt.% this equals a range of 3.4 wt.% to 27.2 wt.% CO₂ in the flue gas. This also equals 15% to 120% of the original CO₂ mass concentration of 22.65 wt.%. The change in CO₂ was offset by a change in N₂ concentration.

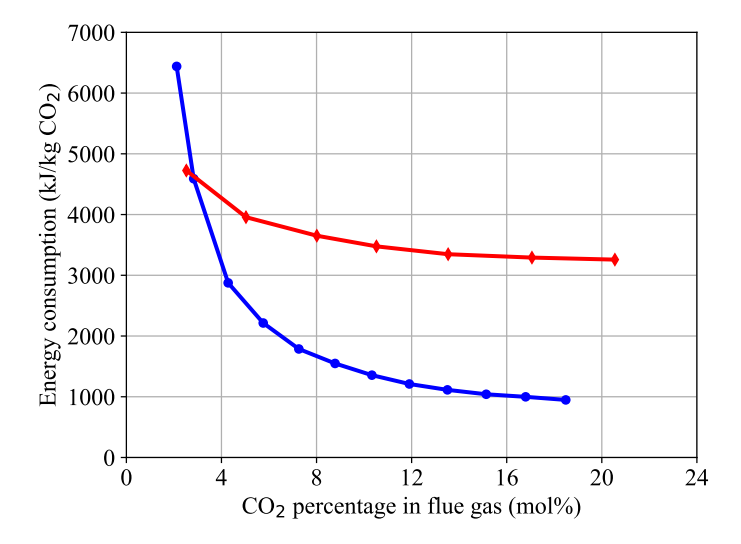


Figure 5.4: Energy required per kg CO₂ captured for HPC and MEA systems as a function of CO₂ concentration at 90% capture rate.

It can be seen in Figure 5.4, that the HPC system generally has a much steeper slope, the import of which is further increased when the difference in magnitudes are considered. It is particularly noticeable at the very lowest CO₂ percentages, where the HPC system consumes a large amount of power per kg CO₂, likely due to it being on the verge of no longer being able to capture 90% of the CO₂ content with this system configuration. This could likely be mitigated to some degree by increasing the pressure difference between the absorber and regenerator, to increase the concentration difference between rich and lean absorbent in the absorber and regenerator, as this would skew the equilibrium difference between them further and increase the rates of reaction. Furthermore, an increase in the absorber pressure would increase the partial CO₂ pressure, increasing the amount of CO₂ dissolved in the solvent and thus increasing the rate of reaction.

Overall, it appears that the HPC system is more efficient comparative to the MEA system at higher CO₂ percentages, although they both retain good performance over most of the range.

To investigate whether the cooling requirements of the HPC system, which are not included in Figure 5.4 above, could have an effect on the range in which the HPC system appears to perform the best, the cooling requirements are shown below in Figure 5.5 alongside the power consumption.

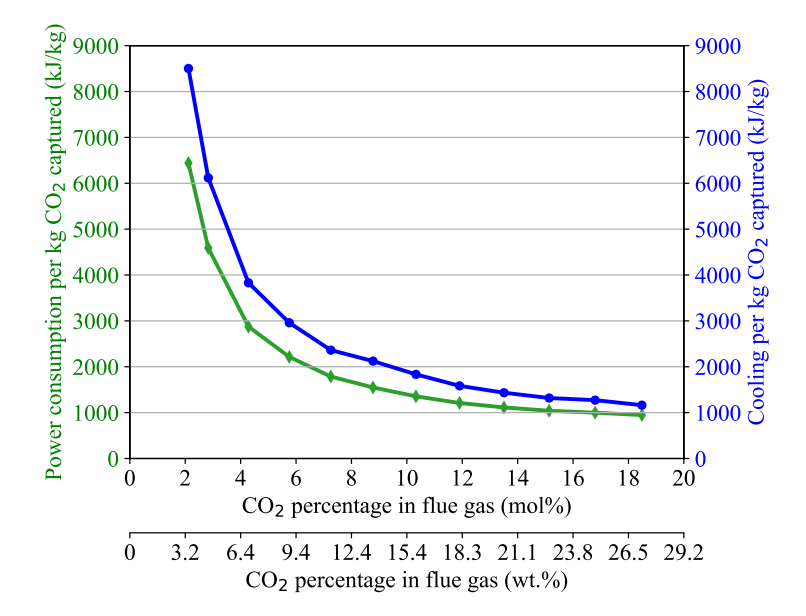


Figure 5.5: Power and cooling required per kg CO₂ captured as a function of CO₂ concentration at 90% capture rate.

As can be seen, the cooling requirements appear to follow the power consumption fairly well. This fits what was also observed previously in this section in Figure 5.3.

5.2.2 Effect of Absorber and Regenerator pressure on System Efficiency

To ascertain whether a higher pressure difference between the absorber and regenerator would be beneficial for the system, both are tested individually. The tests are at a 90% capture rate, and utilize the coal power flue gas shown in Table 5.1 above. The results can be seen below in Figure 5.6 and Figure 5.7, both of which have two y-axes, the leftmost axes along with the green lines being the power consumption per kg CO₂, while the rightmost axes along with the blue lines being cooling per kg CO₂ consumed. Both y-axes on each of the two figures are equal in scale, but have shifted ranges. The pressures are measured at the gas outlets of the columns.

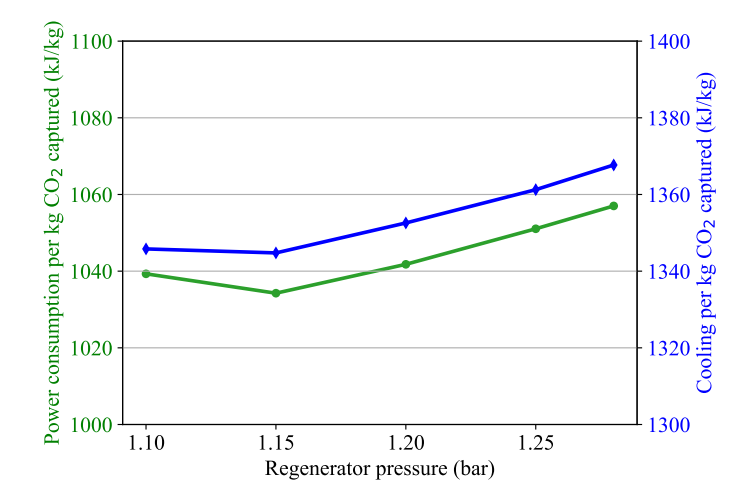


Figure 5.6: Power and cooling per kg CO₂ captured, as a function of regenerator pressure at 90% capture rate, with the blue line being power and green line being cooling

On Figure 5.6 the power and cooling requirements can be seen as a function of the regenerator pressure. As can be seen on the axes, the overall impact on the efficiency from varying the regenerator pressure is very low, but it does appear that there would be a small benefit of lowering it slightly. The change in the graphs below 1.15 bar, are likely due to the system having to be tweaked at 1.1 bar to ensure the CO₂ output stream did not fall below 1 atm from pressure loses. This was done by adding a compressor to the CO₂ outlet of the system, to increase the pressure by 0.05 bar, which offset any power savings. Overall, the biggest benefit over lowering the absorber pressure would likely be a higher rate of reaction within the regenerator.

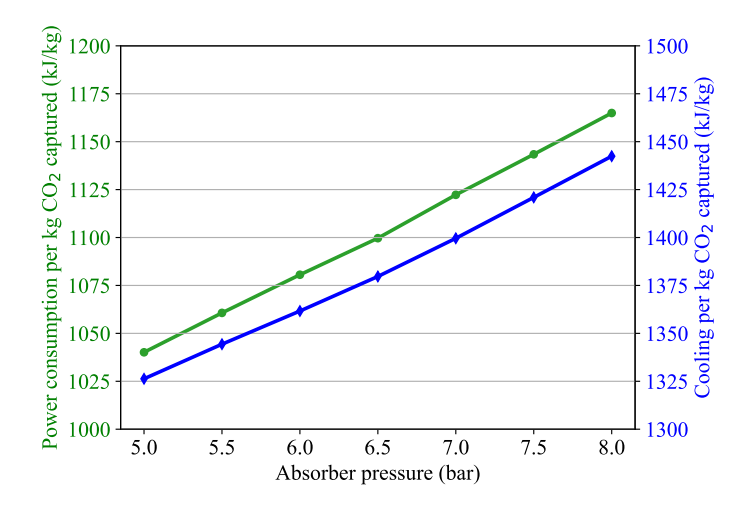


Figure 5.7: Power and cooling per kg CO₂ captured, as a function of absorber pressure at 90% capture rate, with the blue line being power and green line being cooling

On Figure 5.7 the power and cooling requirements can be seen as a function of the absorber pressure. It can be seen that both the power consumed and cooling required increase with increasing absorber pressure, this is likely due to the flue gas being compressed additionally to reach the higher pressures. This shows that, at higher CO₂ concentrations, it is beneficial for the system efficiency to minimize the absorber pressure. Lesser pressure does, however, also increase the size of the system, as it decreases the rate of reaction. It may, therefore, in reality be beneficial to increase the pressure to lessen the absorber footprint and CAPEX. This could, as mentioned previously, especially be true for lower CO_2 concentrations, as the system at 5 bar had difficulty reaching 90% capture rate at lower concentrations. This can be seen in Figure 5.4, where the power consumption increases drastically at low concentrations. This high power consumption could potentially be lowered, if the absorber pressure was higher, as this would increase the partial CO₂ pressure in the the absorber. This is therefore tested, as can be seen below in Figure 5.8, which is made using a CO₂ concentration of 6 wt.% in the flue gas, similar to the natural gas power flue gas.

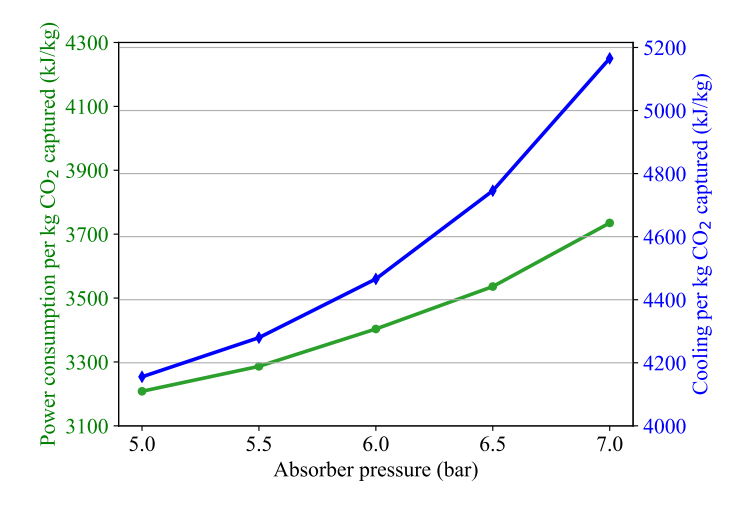


Figure 5.8: Power and cooling per kg CO₂ captured, as a function of absorber pressure at 90% capture rate and low CO₂ concentration, with the blue line being power and green line being cooling

As can be seen, even at lower CO_2 pressures, increasing the absorber pressure still does not decrease the power consumption as theorized, and the increase in power consumption is, in fact, larger percentage wise than at the high CO_2 concentration from 5 to 7 bar. Interestingly enough, however, the curve seen in Figure 5.7 is much more pronounced here.

5.2.3 Effect of Flue Gas Mass Flow on System Efficiency

As showcased in Section 5.2.1, a change in the amount of CO_2 that enters the CO_2 capture system can affect its efficiency. Another way this can occur is when the total mass flow into the system changes, such as when the CO_2 source the system is connected to changes its load. This will, therefore, be investigated in this section.

Below, in Figure 5.9 and 5.10, the power consumption and cooling requirements per kg CO_2 captured can be seen, both as a function of varying flue gas mass flow rate. Both figures are taken at a 90% capture rate, which was achieved by adjusting the lean flash box pressure.

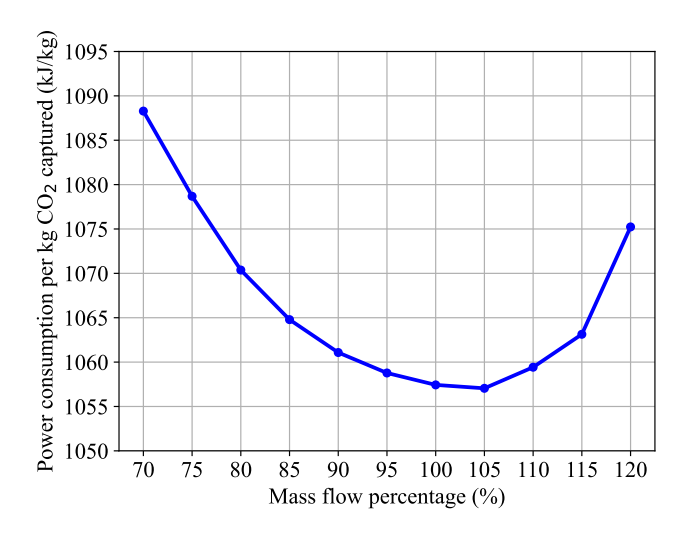


Figure 5.9: Power per kg CO₂ captured as a function of changing of flue gas mass flow with constant CO₂ concentration at 90% capture rate

It can be seen on Figure 5.9 that the basis mass flow, which is approximately 1/10 of the solvent liquid flow rate, appears to perform very well with the current configuration, having almost equal consumption to the case with 105% mass flow, which is marginally the highest efficiency case. Important to note, however, is the y-axis on this model, which goes from 1050 to 1095 kJ/kg CO₂. This shows, that the overall efficiency loss when varying the flue gas mass flow is a few percentage points within the range examined here. Interesting enough, however, the systems cooling requirements does not seem to fully follow the power consumption in this case, as it did previously. This can be seen when comparing Figure 5.9 and 5.10, as in Figure 5.10, the flue gas curve does not bottom out until a mass flow of 115%, which is ten percentage points higher than the power consumption. Furthermore, as can be seen on Figure 5.10, the change in cooling requirements per kg CO₂ increase magnitudes more than the power consumption does. This is not because the cooling requirements does not decrease along with the mass flow, simply that it does not decrease nearly fast enough to retain a constant, or near constant, ratio

of cooling to incoming flue gas.

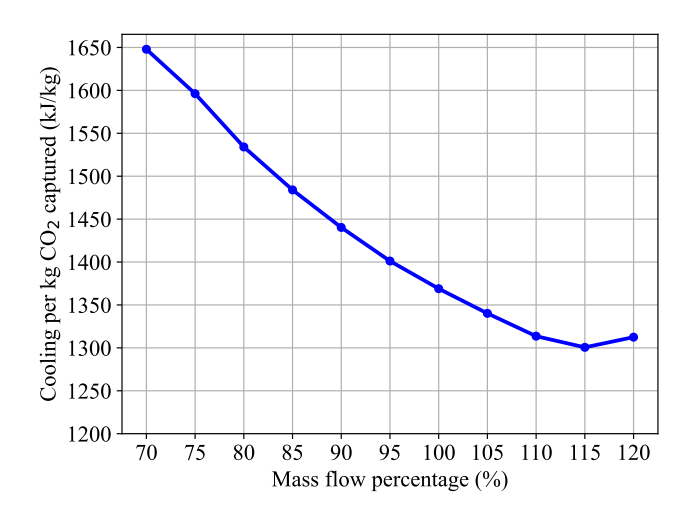


Figure 5.10: Cooling required per kg CO₂ captured as a function of changing of flue gas mass flow with constant CO₂ concentration at 90% capture rate

Overall, Figure 5.9 and 5.10 indicate that the current flue gas mass flow, or potentially a slightly higher one to decrease cooling requirements per kg CO₂, would be optimal. Furthermore, the overall cooling requirements does get reduced as the mass flow decreases, so running the system despite having a decreased flue gas mass flow into the system appears to still be viable, which as, mentioned earlier, is beneficial for power plants or factories that vary their load and thus flue gas mass flow output.

Another important case, may be industries that vary the overall mass flow of their flue gas while retaining a constant CO₂ mass flow. This mainly applies to systems that control boiler temperatures by varying the air flow into the combustion chamber. This was simulated and the results can be seen below in Figure 5.11 and 5.12. In the figures, the power consumption and cooling requirements for the system shown as function of the flue gas mass flow at 90% capture rate. As mentioned above, the overall CO₂ flow rate into the system was kept constant, while the total mass flow of the flue gas stream was changed, this was achieved by increasing CO₂ and O₂ concentration in the flue gas as the mass flow increased, to simulate more atmospheric air entering. The results of this can be seen on the x-axes of the Figures, where both the CO₂ wt.% and the percent flue gas mass flow is shown. The flue gas mass flow is based on 100% mass flow being the flue gas mass flow at a 10 to 1 solvent to flue gas mass flow ratio.

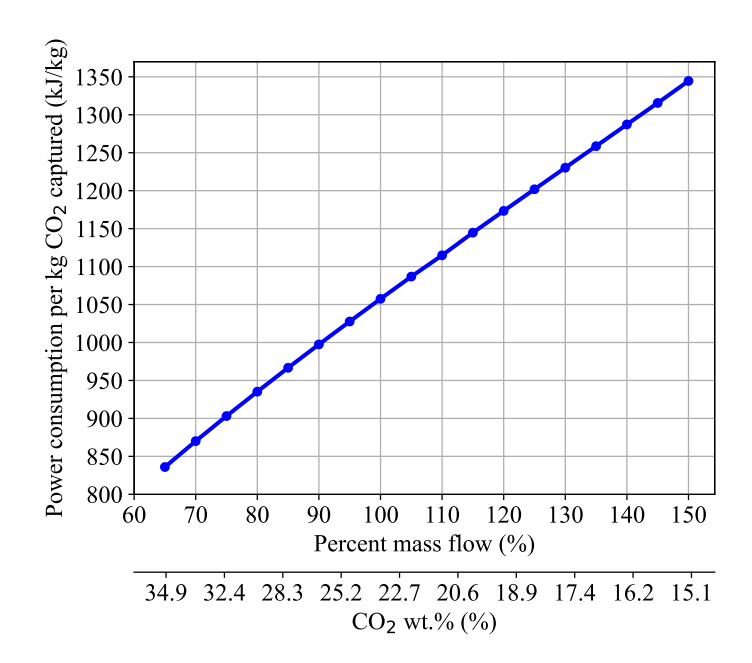


Figure 5.11: Power per kg CO_2 captured as a function of changing of flue gas mass flow with constant CO_2 mass flow at 90% capture rate

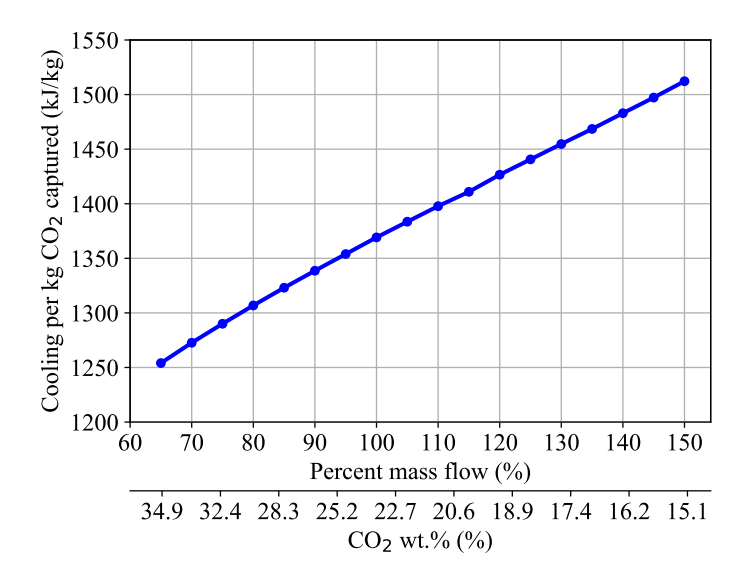


Figure 5.12: Cooling required per kg CO_2 captured as a function of changing of flue gas mass flow with constant CO_2 mass flow at 90% capture rate

Figure 5.11 and 5.12 show that both the power consumption and cooling requirements increase close to linearly over this range, with a slight curve indicating the increase in power and cooling required will decrease with decreasing CO_2 concentrations. The contrast between these two figures and Figure 5.9 and 5.10 is

apparent, as there is no point where Figure 5.9 and 5.10 has decreasing power or cooling per kg CO₂ captured as a function of increasing flue gas mass flow. This does, however, showcase the fact that in both cases, the total power consumption and cooling requirements increase as a function of the flue gas mass flow. The difference being, that as the CO₂ mass flow does not increase along with the flue gas mass flow in this case, the power consumed per kg CO₂ captured increases proportionally with the total power consumed. The opposite of this can, of course, be seen in the cases showcased in Figure 5.11 and 5.12, where the CO₂ mass flow does increase along with the flue gas mass flow, therefore reducing the power consumed and cooling required per kg CO₂ compared to Figure 5.9 and 5.10.

5.2.4 Effects of Flash Box Pressure and Steam Temperature on Capture Rate and System Efficiency

In the report by M.B. Jeppesen [30], it was proposed that this type of HPC system could be controlled solely with the pressures in the flash boxes. In the making of this report this was, however, put to question, as the flash boxes are very sensitive to changes in pressure, which means that to control the system using flashboxes, very precise pressure control would be required.

As the flashboxes are a core part of this systems function and energy efficiency, this could have an impact on the system performance. This issue will, therefore, be explored along with a potential solution being proposed. below in Figure 5.13, the correlation between the pressure in the lean flash box and the capture rate of the system is shown. As can be seen, a change of 0.005 bars changes the overall capture rate in wt.% by one percentage point.

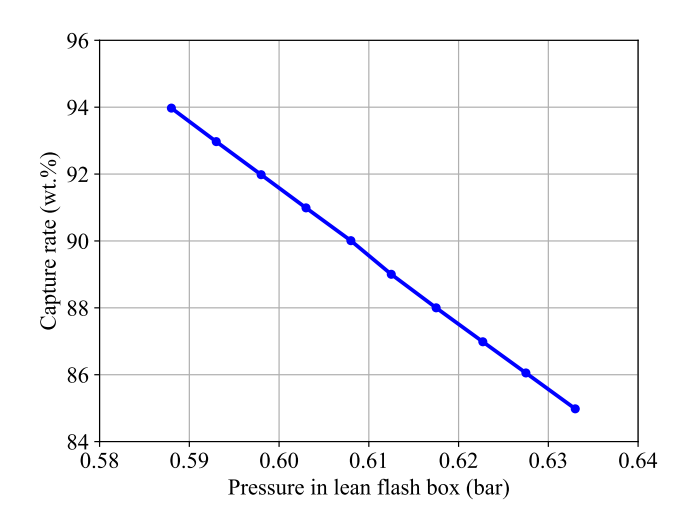


Figure 5.13: Figure showing the wt.% capture rate (vertical axis) as a function of the pressure in the lean flash box (horizontal axis)

An alternative solution might, therefore, be to place a heater on the lean flash box steam output, this heater would operate in the temperature interval of 90 $^{\circ}$ C to 110 $^{\circ}$ C and could be supplied by excess heat in the system, although this will redirect some energy from the pre-expansion flue gas heater thus reducing the systems power recuperation. The correlation between the capture rate and lean flash bot heater temperature increase, can be seen in Figure 5.14 below.

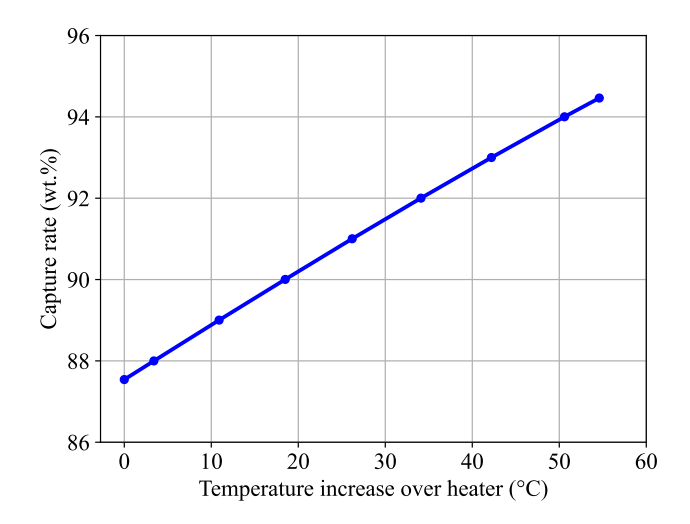


Figure 5.14: Figure showing the wt.% capture rate (vertical axis) as a function of the temperature increase over the lean flash box steam heater (horizontal axis)

As can be seen, an increase in the capture rate by one percentage point requires a temperature increase of 7.4 °C to 8.7 °C in the flash box steam, increasing as a function of the temperature over the steam heater. This corresponds with an energy requirement of $47.4 \frac{kJ}{kg\text{CO}_2\cdot\%}$ in the heater at low temperature increases. If the heater were to be a heat exchanger exchanging heat with the pressurized rich flue gas, as seen previously in the pinch point analysis in Figure 5.2, it can be calculated how big a change in mass flow is needed to change the capture rate by one percentage point. Thereby, a comparison can be made between controlling the system with the flash box pressure, and controlling it using a heater on the flash box steam output.

The calculations are made using the coal power plant flue gas, which has a heat capacity of approximately 1 $\frac{kJ}{kg \cdot K}$ at constant pressure at 5 bar [47]. The approximate mass flow of flue gas per percentage point would, therefore, be 44.7 $\frac{kg(Flue)}{kg(CO_2) \cdot C}$ per percentage point change in capture rate. If the pinch point analysis is taken into account, where the temperature of the flue gas decreases by approximately 22 °C while exchanging heat with the flash box heater, which increased the steam temperature by 20 °C, the flue gas mass flow to the heat exchanger becomes 2.15 $\frac{kg(Flue)}{kg(CO_2)}$ per percentage point. This is compared to the 0.005 bars change per per-

centage point in the flash box, which also has a significantly higher mass flow than the heat exchanger, as the entire lean sorbent flow of the systems flows through the lean flash box. In return, however, there is a reduction in system efficiency as mentioned previously, as while the heater allows for higher lean flash box pressures, thereby reducing the pump and compressors power consumption, the flue gas used to heat the heat exchanger could instead be used to recuperate power in the flue gas expander. This can be seen below in Figure 5.15. It is worth noting that the right and left axis are equal in scale, but have shifted ranges.

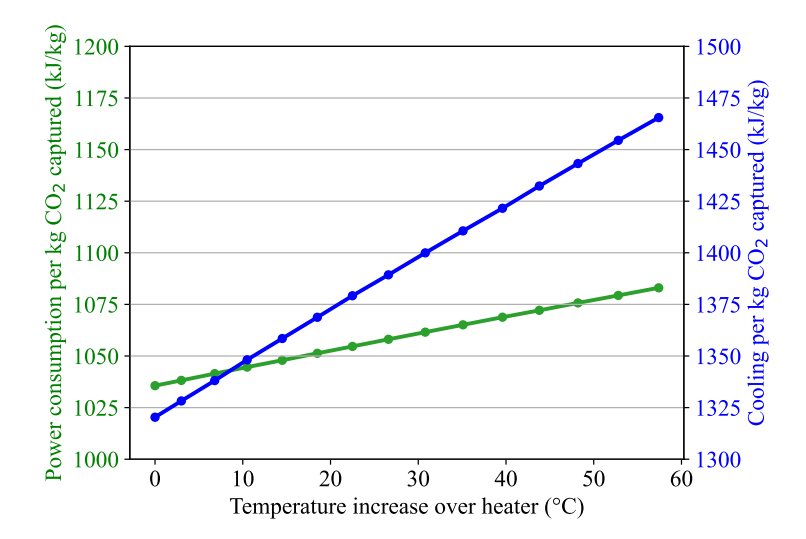


Figure 5.15: Figure showing the change in power consumption (green line, left axis) and cooling requirement (blue line, right axis) per degree celsius temperature increase over the flash box steam heater (bottom axis).

As can be seen, both the systems overall cooling requirement and power consumption increase with increased heater duty, which means the potential ease of control comes at a cost of efficiency, and limiting the heating duty of the heat exchanger, potentially solely using it for fine control, is desirable.

5.3 Table of Recommended Settings

In this section, the optimizations found in this project are all gathered and a table of recommended settings of the HPC system can be seen at various operating conditions. The table was based on the coal power flue gas at a 90% capture rate in wt.%, with various CO_2 concentrations.

CO ₂ Concentration (wt.%)	Lean flash pressure (bar)	Cond. flash pressure 1 (bar)	Cond. flash pressure 2 (bar)	Reboiler duty (kJ/kg CO ₂)	Absorber pressure low (bar)	Regenerator pressure low (bar)	Power consumption (kJ/kg CO ₂)	Cooling requirement (kJ/kg CO ₂)
26	0.508	0.32	0.27	750	5	1.15	896	961
24	0.538	0.36	0.31	750	5	1.15	915	993
22	0.56	0.4	0.35	750	5	1.15	956	1053
20	0.595	0.4	0.35	750	5	1.15	1077	1350
18	0.632	0.4	0.35	750	5	1.15	1159	1474
16	0.667	0.4	0.35	750	5	1.15	1268	1636
14	0.697	0.4	0.35	750	5	1.15	1418	1853
12	0.708	0.4	0.35	750	5	1.15	1637	2163
10	0.71	0.4	0.35	750	5	1.15	1919	2487
8	0.709	0.4	0.35	750	5	1.15	2408	3146
6	0.702	0.4	0.35	750	5	1.15	3277	4298

Table 5.2: Table of recommended system settings for various flue gas CO₂ concentrations, "low" in absorber and regenerator pressure refers to it being the lowest pressure in the column (gas outlet)

Chapter 6

Conclusion

The aim of this project, was to investigate the effects of varying operating conditions on a hot potassium carbonate (HPC) carbon capture system, to find the range of conditions in which this system excels, both in regards to power consumption and utility requirements. To achieve this goal, a rate based, numerical model of an electrified HPC system was made in Aspen Plus V12.1, as seen in Chapter 4. This model was validated by comparing the results of the absorber to experimental data, with the model results diverging by 14% to 17% from the experimental data at 90 °C and 110 °C. A divergence from expected results was observed above 110 °C, and the model was determined to have a temperature limit of 120 °C for kinetic calculations, as higher temperatures would exceed a 5% divergence from expected results.

In Section 5.1, it was explored what utility requirements were present for the system and it was determined that the system does not require any hot utility if adjusted correctly, but did require 1330 kJ/kg CO_2 of cold utility in the case simulated, to cool streams between 35 °C and 90 °C.

In Section 5.2.1, the effects of varying flue gas compositions were investigated. It was discovered that both the power consumption and cooling requirements are inversely proportional to the CO_2 concentration in the flue gas and that compared to an MEA system, the HPC system appears to be more sensitive to changes in flue gas CO_2 concentration, having much higher energy consumption increases at low CO_2 concentrations. This suggests that the HPC system is more suited to operate with high CO_2 concentration flue gas streams.

It was then theorized, that a change in the pressure difference between the absorber and regenerator may increase the systems performance, particularly at low CO_2 concentrations, thus increasing the viable range of the system. An investigation into the absorber and regenerator pressures' effects on the system was carried out in Section 5.2.2. Here it was discovered that with a CO_2 wt.% of 22.65%, lowering the regenerator pressure from 1.28 bar to 1.15 bar slightly decreased the power

and cooling requirements, whereas increasing the absorber pressure resulted in both parameters increasing. The absorber pressure variation was then tested at a low flue gas CO_2 concentration, but was once again found to increase power and cooling requirements, disproving the theory that it would be beneficial at lower CO_2 concentrations.

In Section 5.2.3, varying flue gas mass flow was tested, it was found that a flue gas mass flow of approximately 1/10th of the total sorbent liquid flow was optimal for power efficiency, with an absorbent concentration of 0.25 wt.%, but slightly higher flue gas mass flows was optimal for decreasing cooling requirements. Furthermore, with a constant CO₂ flow but varying total flue gas mass flow, the power and cooling requirements will increase, as the mass flow increases.

Finally, the flash boxes effect on the systems capture rate and efficiency was investigate in Section 5.2.4, mainly to investigate the sensitivity of the flash boxes. It was discovered that a 0.005 bar change to the lean flash box pressure would change the system capture rate by approximately one percentage point wt.%, whereas a steam heater attached to the lean flash box steam output, would require a 7.4 $^{\circ}$ C to 8.7 $^{\circ}$ C temperature increase for the same change in capture rate. This would potentially increase the level of control of the system, at the cost of a slight decrease in system efficiency.

The aim of the project was therefore accomplished, as various operating conditions have been investigated, along with some potential changes to the internal systems, to find performance of the system under varying operating conditions, as well as where the system would perform the best. A table was set up in Section 5.3 of recommended system settings at various flue gas CO₂ concentrations, to reflect the optimizations found in this project.

- [1] The NOAA Annual Greenhouse Gas Index (AGGI). NOAA Global Monitoring Laboratory. 2023. URL: https://gml.noaa.gov/aggi/aggi.html (visited on 02/12/2023).
- [2] Hannah Ritchie and Max Roser. CO_2 emissions. Our World in Data. 2024. URL: https://ourworldindata.org/co2-emissions (visited on 02/12/2023).
- [3] "Climate Change 2023: Synthesis Report". In: (2023). Contribution of Working Groups I, II and III to the Sixth Assessment Report of the Intergovernmental Panel on Climate Change, pp. 35–115. DOI: 10.59327/IPCC/AR6-9789291691647.
- [4] Loiy Al-Ghussain. "Global warming: review on driving forces and mitigation". In: *Environmental Progress & Sustainable Energy* 38.1 (2019), pp. 13–21. DOI: 10.1002/ep.13041.
- [5] V. Ramanathan and Y. Feng. "Air pollution, greenhouse gases and climate change: Global and regional perspectives". In: *Atmospheric Environment* 43.1 (2009). Atmospheric Environment Fifty Years of Endeavour, pp. 37–50. ISSN: 1352-2310. DOI: 10.1016/j.atmosenv.2008.09.063.
- [6] *The Paris Agreement*. Paris Climate Change Conference, COP 21. United Nations Framework Convention on Climate Change, 2015. T.I.A.S. No. 16-1104.
- [7] What is The Paris Agreement? United Nations Framework Convention on Climate Change. 2024. URL: https://unfccc.int/process-and-meetings/the-paris-agreement (visited on 02/09/2024).
- [8] Yuxin Wu et al. "Recent advances in carbon dioxide capture and utilization with amines and ionic liquids". In: *Green Chemical Engineering* 1.1 (2020), pp. 16–32. DOI: 10.1016/j.gce.2020.09.005. URL: https://www.sciencedirect.com/science/article/pii/S2666952820300054.
- [9] Prakashpathi Gunasekaran, Amornvadee Veawab, and Adisorn Aroonwilas. "Corrosivity of Amine-Based Absorbents for CO2 Capture". In: *Energy Procedia* 114 (2017). 13th International Conference on Greenhouse Gas Control Technologies, GHGT-13, 14-18 November 2016, Lausanne, Switzerland,

- pp. 2047-2054. ISSN: 1876-6102. DOI: https://doi.org/10.1016/j.egypro. 2017.03.1339.
- [10] Mohammad R.M. Abu-Zahra et al. "CO2 capture from power plants: Part I. A parametric study of the technical performance based on monoethanolamine". In: International Journal of Greenhouse Gas Control 1 (2007), pp. 37–46. DOI: https://doi.org/10.1016/S1750-5836(06)00007-7. URL: https://www.sciencedirect.com/science/article/pii/S1750583606000077.
- [11] Kazuya Goto et al. "Potential of Amine-based Solvents for Energy-saving CO2 Capture from a Coal-fired Power Plant". In: *Journal of the Japan Institute of Energy* 95 (2016), pp. 1133–1141. URL: https://www.jstage.jst.go.jp/article/jie/95/12/95_1133/_pdf.
- [12] Technology readiness levels (TRL). Horizon 2020. 2020. URL: https://ec.europa.eu/research/participants/data/ref/h2020/wp/2014_2015/annexes/h2020-wp1415-annex-g-trl_en.pdf (visited on 10/23/2023).
- [13] State of The Art: CCS Technologies 2023. Global CCS Institute. 2023. URL: https://www.globalccsinstitute.com/wp-content/uploads/2023/08/State-of-the-Art-CCS-Technologies-2023-GCCSI-Final.pdf (visited on 02/14/2024).
- [14] Yuhua Duan et al. "Ab Initio Thermodynamic Study of the CO2 Capture Properties of Potassium Carbonate Sesquihydrate, K2CO3·1.5H2O". In: *The Journal of Physical Chemistry C* 116.27 (2012), pp. 14461–14470. DOI: 10.1021/jp303844t.
- [15] S. J. Harjac et al. "Influence of solution chemistry and surface condition on the critical inhibitor concentration for solutions typical of hot potassium carbonate CO2 Removal Plant". In: *Journal of Materials Science* 42.18 (2007), 7762–7771. DOI: 10.1007/s10853-007-1613-y.
- [16] Carbon capture from Biomass plants. Capsol. 2023. URL: https://www.capsoltechnologies.com/biomass (visited on 12/04/2023).
- [17] Capsol EoP®. Capsol. 2023. URL: https://www.capsoltechnologies.com/capsol-eop (visited on 10/23/2023).
- [18] Bluenzyme. Saipem. 2024. URL: https://www.saipem.com/en/solutions-energy-transition/reduce-co2-emissions/co2-capture-storage/carbon-capture/bluenzyme (visited on 02/14/2024).
- [19] Uffe Ditlev Bihlet et al. "Extended Abstract: The ConsenCUS Project: Carbon Neutral clusters by Electricity-based Innovations in Capture, Utilisation and Storage". In: 16th International Conference on Greenhouse Gas Control Technologies (2022). DOI: 10.2139/ssrn.4297064.

[20] Gianluca Valenti, Davide Bonalumi, and Ennio Macchi. "A parametric investigation of the Chilled Ammonia Process from energy and economic perspectives". In: Fuel 101 (2012). 8th European Conference on Coal Research and Its Applications, pp. 74–83. DOI: https://doi.org/10.1016/j.fuel. 2011.06.035. URL: https://www.sciencedirect.com/science/article/pii/S001623611100353X.

- [21] Chilled Ammonia Process. Baker Hughes. 2023. URL: https://www.bakerhughes.com/process-solutions/chilled-ammonia-process (visited on 10/23/2023).
- [22] Luca Riboldi and Olav Bolland. "Overview on Pressure Swing Adsorption (PSA) as CO2 Capture Technology: State-of-the-Art, Limits and Potentials". In: *Energy Procedia* 114 (2017). 13th International Conference on Greenhouse Gas Control Technologies, GHGT-13, 14-18 November 2016, Lausanne, Switzerland, pp. 2390–2400. ISSN: 1876-6102. DOI: 10.1016/j.egypro.2017.03.1385.
- [23] Jian-Bin Lin et al. "A scalable metal-organic framework as a durable physisorbent for carbon dioxide capture". In: *Science* 374.6574 (2021), pp. 1464–1469. DOI: 10.1126/science.abi7281. URL: https://www.science.org/doi/abs/10.1126/science.abi7281.
- [24] Meet the Svante Carbon Capture Ecosystem. Svante. 2024. URL: https://www.svanteinc.com/carbon-capture-technology/(visited on 02/15/2024).
- [25] Medhat A. Nemitallah et al. "Oxy-fuel combustion technology: current status, applications, and trends". In: *International Journal of Energy Research* 41.12 (2017), pp. 1670–1708. DOI: https://doi.org/10.1002/er.3722.
- [26] Howoun Jung et al. "Dynamic Modeling and Analysis of Amine-based Carbon Capture Systems". In: *IFAC-PapersOnLine* 51.18 (2018). 10th IFAC Symposium on Advanced Control of Chemical Processes ADCHEM 2018, pp. 91–96. ISSN: 2405-8963. DOI: 10.1016/j.ifacol.2018.09.263.
- [27] Sanoja A. Jayarathna, Bernt Lie, and Morten C. Melaaen. "Amine based CO2 capture plant: Dynamic modeling and simulations". In: *International Journal of Greenhouse Gas Control* 14 (2013), pp. 282–290. ISSN: 1750-5836. DOI: https://doi.org/10.1016/j.ijggc.2013.01.028.
- [28] Rana Prathap Padappayil and Judith Borger. *Ammonia Toxicity*. 2023. URL: https://www.ncbi.nlm.nih.gov/books/NBK546677/ (visited on 02/21/2024).
- [29] Stellan Hamrin. "Method and plant for CO2 capture". Pat. Capsol-EoP A/S, US10391447B2. 2019.
- [30] Mads Bluhme Jeppesen. Heat Integration and Optimization of Post-Combustion Hot Potassium Carbonate Carbon Capture. Student Report. 2024.
- [31] Hussein K. Abdel-Aal, Mohamed A. Aggour, and Mohamed A. Fahim. *Petroleum and Gas Field Processing*. 1st ed. CRC Press, 2003. ISBN: 9780429258497.

[32] David W Savage, Gianni Astarita, and Shriram Joshi. "Chemical absorption and desorption of carbon dioxide from hot carbonate solutions". In: *Chemical Engineering Science* 35.7 (1980), pp. 1513–1522.

- [33] Tohid Nejad Ghaffar Borhani et al. "Rate-based simulation and comparison of various promoters for CO2 capture in industrial DEA-promoted potassium carbonate absorption unit". In: Journal of Industrial and Engineering Chemistry 22 (2015), pp. 306–316. ISSN: 1226-086X. DOI: 10.1016/j.jiec.2014.07.024. URL: https://www.researchgate.net/publication/262185358.
- [34] modified Arrhenius equation. 2019. DOI: 10.1351/goldbook.M03963. URL: https://doi.org/10.1351/goldbook.M03963.
- [35] George Bollas, Chau-Chyun Chen, and P. Barton. "Refined electrolyte-NRTL model: Activity coefficient expressions for application to multi-electrolyte systems". In: *AIChE Journal* 54 (2008), pp. 1608 –1624. DOI: 10.1002/aic. 11485.
- [36] Chau-Chyun Chen and Yuhua Song. "Generalized electrolyte-NRTL model for mixed-solvent electrolyte systems". In: *AIChE Journal* 50.8 (2004), 1928–1941. DOI: 10.1002/aic.10151.
- [37] Acid Gas Cleaning in Aspen HYSYS®. Aspentech. 2017. URL: https://www.aspentech.com/en/resources/jump-start-guide/acid-gas-cleaning-in-aspen-hysys (visited on 10/27/2023).
- [38] B. R. Pinsent, L. Pearson, and F. J. Roughton. "The kinetics of combination of carbon dioxide with hydroxide ions". In: *Transactions of the Faraday Society* 52 (1956), 1512–1520. DOI: 10.1039/tf9565201512.
- [39] T. J. Edwards et al. "Vapor-liquid equilibria in multicomponent aqueous solutions of volatile weak electrolytes". In: *AIChE Journal* 24.6 (1978), 966–976. DOI: 10.1002/aic.690240605.
- [40] J. S. Tosh et al. "Equilibrium study of the system potassium carbonate, potassium biocarbonate, carbon dioxide, and water". In: *Bureau of Mines, Report of investigations* 5484 (1959).
- [41] Anusha Kothandaraman. Carbon Dioxide Capture by Chemical Absorption: A Solvent Comparison Study. 2010. URL: http://hdl.handle.net/1721.1/59877 (visited on 08/12/2025).
- [42] Henrik Lund et al. "4th Generation District Heating (4GDH): Integrating smart thermal grids into future sustainable energy systems". In: Energy 68 (2014), pp. 1–11. ISSN: 0360-5442. DOI: https://doi.org/10.1016/j.energy. 2014.02.089. URL: https://www.sciencedirect.com/science/article/pii/S0360544214002369.

[43] David M. Austgen et al. "Model of vapor-liquid equilibria for aqueous acid gas-alkanolamine systems using the electrolyte-NRTL equation". In: *Industrial & Engineering Chemistry Research* 28.7 (1989), 1060–1073. DOI: 10.1021/ie00091a028.

- [44] Fatih Güleç, Will Meredith, and Colin E. Snape. "Progress in the CO2 Capture Technologies for Fluid Catalytic Cracking (FCC) Units—A Review". In: Frontiers in Energy Research Volume 8 2020 (2020). ISSN: 2296-598X. DOI: 10. 3389/fenrg.2020.00062. URL: https://www.frontiersin.org/journals/energy-research/articles/10.3389/fenrg.2020.00062.
- [45] Wouter Schakel et al. "Impact of fuel selection on the environmental performance of post-combustion calcium looping applied to a cement plant". In: *Applied Energy* 210 (Jan. 2018), pp. 75–87. DOI: 10.1016/j.apenergy.2017. 10.123.
- [46] Jo Husebye et al. "Techno Economic Evaluation of Amine based CO2 Capture: Impact of CO2 Concentration and Steam Supply". In: *Energy Procedia* 23 (2012). The 6th Trondheim Conference on CO2 Capture, Transport and Storage, pp. 381–390. ISSN: 1876-6102. DOI: https://doi.org/10.1016/j.egypro.2012.06.053.
- [47] AspenTech. AspenPlus® V12.1. URL: https://www.aspentech.com.